Agricultural and Forest Meteorology 307 (2021) 108465

Contents lists available at ScienceDirect

Agricultural and Forest Meteorology

journal homepage: www.elsevier.com/locate/agrformet

Soil greenhouse gas emissions from a sisal chronosequence in Kenya

Sheila Wachiye [a,b,e,*], Lutz Merbold [b,f], Timo Vesala [c,g,h], Janne Rinne [d], Sonja Leitner [b], Matti Räsänen [a,c], Ilja Vuorinne [a], Janne Heiskanen [a], Petri Pellikka [a]

[a] Earth Change Observation Laboratory, Department of Geosciences and Geography, University of Helsinki, Finland
[b] Mazingira Centre, International Livestock Research Institute (ILRI), P.O. Box 30709, 00100 Nairobi Kenya
[c] Institute for Atmospheric and Earth System Research/Physics, Faculty of Science, University of Helsinki
[d] Department of Physical Geography and Ecosystem Science, Lund University, Sweden
[e] School of Natural Resources and Environmental Management, University of Kabianga, Kenya
[f] Agroscope, Research Division Agroecology and Environment, Reckenholzstrasse 191, 8046 Zurich, Switzerland
[g] Institute for Atmospheric and Earth System Research/Forest Sciences, Faculty of Agriculture and Forestry, University of Helsinki, Finland
[h] Yugra State University, 628012, Khanty-Mansiysk, Russia

ARTICLE INFO

Keywords:
Soil moisture
Carbon dioxide (CO_2)
Nitrous oxide (N_2O)
Methane (CH_4)
Sub-Saharan Africa
Land-use change, Static chamber

ABSTRACT

Sisal (*Agave sisalana*) is a climate-resilient crop grown on large-scale farms in semi-arid areas. However, no studies have investigated soil greenhouse gas (GHGs: CO_2, N_2O and CH_4) fluxes from these plantations and how they relate to other land cover types. We examined GHG fluxes (Fs) in a sisal chronosequence at Teita Sisal Estate in southern Kenya. The effects of stand age on Fs were examined using static GHG chambers and gas chromatography for a period of one year in seven stands: young stands aged 1–3 years, mature stands aged 7–8 years, and old stands aged 13–14 years. Adjacent bushland served as a control site representing the surrounding land use type. Mean CO_2 fluxes were highest in the oldest stand (56 ± 3 mg C m^{-2} h^{-1}) and lowest in the 8-year old stand (38 ± 3 mg C m^{-2} h^{-1}), which we attribute to difference in root respiration between the stand. All stands had 13–28% higher CO_2 fluxes than bushland (32 ± 3 mg C m^{-2} h^{-1}). CO_2 fluxes in the wet season were about 70% higher than dry season across all sites. They were influenced by soil water content (W_S) and vegetation phenology. Mean N_2O fluxes were very low (<5 μg N m^{-2} h^{-1}) in all sites due to low soil nitrogen (N) content. About 89% of CH_4 fluxes were below the detection limit (LOD ± 0.02 mg C m^{-2} h^{-1}). Our results imply that sisal plantations have higher soil CO_2 emissions than the surrounding land use type, and the seasonal emissions were largely driven by W_S and the vegetation status. Methane and nitrous oxide are of minor importance. Thus, soil GHG fluxes from sisal plantations are a minor contributor to agricultural GHG emissions in Kenya.

1. Introduction

Greenhouse gas emissions are a major global concern due to their effects on the climate and the resulting environmental and human impacts (IPCC, 2013). The primary greenhouse gases (GHG), carbon dioxide (CO_2), methane (CH_4) and nitrous oxide (N_2O), have been the focus of many studies over the last decades (Muñoz et al., 2010). This is due to the continuous increase in the concentration of these gases in the atmosphere, causing climate change, which is sequentially leading to unprecedented effects on ecosystems, including the tropics and subtropics (IPCC, 2013). Anthropogenic soil management within agriculture has been identified to further contribute to increasing GHG emissions in the atmosphere (Smith et al., 2003), but *in situ* data for agro-ecosystems in sub-Saharan Africa remain scarce.

Soil GHG fluxes (F_S) have mostly been attributed to microbial and plant processes in the soil (Oertel et al., 2016). The rates of soil–atmosphere GHG exchange depend on environmental factors such as climate, vegetation type and soil properties (Raich and Tufekcioglu, 2000; Smith et al., 2003; Wang et al., 2013), with soil temperature (T_S) and soil water content (W_S) as key factors affecting seasonal variations (Carbone et al., 2011; Davidson et al., 1998; Roby et al., 2019). The differences in environmental conditions across different ecosystems can cause substantial differences in F_S in and between different ecosystems (Wang et al., 2013). Therefore, to implement mitigation measures and climate-smart interventions, there is a need to understand the dynamics of F_S and their influential factors at the ecosystem level. Currently, such

* Corresponding author.
E-mail address: sheila.wachiye@helsinki.fi (S. Wachiye).

https://doi.org/10.1016/j.agrformet.2021.108465
Received 16 January 2021; Received in revised form 23 April 2021; Accepted 3 May 2021
Available online 25 May 2021

baseline data are still scarce for many ecosystems in Africa, which hinders the development of targeted climate-smart agricultural activities (Hickman et al., 2014; Valentini et al., 2014).

Stand age is one of the factors found to influence F_S (Klopatek, 2002; Saiz et al., 2006). As vegetation develops, modifications in its structure and physiology affect essential processes that control F_S (Högberg et al., 2001), leading to variations in F_S with stand age (Klopatek, 2002). Considerable research into the effects of stand age on F_S has been reported from forest plantations (Fang et al., 1998; Saiz et al., 2006; Wiseman and Seiler, 2004), as well as oil palm and rubber plantations (Gao et al., 2019; Sigau and Hamid, 2018; Smith et al., 2012). However, only a few studies have investigated soil CO_2 fluxes in tropical plantations (Ewel et al., 1987; Fang et al., 1998; Gao et al., 2019; Sigau and Hamid, 2018). Apart from the fact that these studies have mainly focused on forest plantations, with a clear lack of consideration of other plantation types, even fewer have examined the emissions of all three GHGs (CO_2, N_2O and CH_4), and no such studies to the best of our knowledge have been reported from arid and semi-arid lands (ASAL) in Africa.

To help fill this knowledge gap, this study investigated the effects of stand age on F_S (CO_2, N_2O and CH_4) in a chronosequence of sisal plantations in the ASAL of Southern Kenya. Sisal (*Agave sisalana*) is a perennial herbaceous crop from the *Agavaceae* family native to Mexico (Kimaro et al., 1994). Sisal is drought-tolerant and can be grown in areas with rainfall as low as 600 mm per annum (Li et al., 2000), and is therefore ideal for ASALs that have been branded unsuitable for agriculture (Von Cruz and Dierig, 2015). The crassulacean acid metabolism (CAM) pathway of the sisal plant, featuring night-time uptake of CO_2 and increased water-use efficiency (WUE), provides great potential as a crop to be widely used in a changing climate (Yang et al., 2015). Furthermore, during processing, the organic waste and leaf residues can be used to generate electricity or make ecological housing material (Broeren et al., 2017), and at the end of their life cycle, sisal plants are biodegradable (FAO, 2012). The leaves provide the world's most important hard natural fibre, which is used in the production of twines, ropes, sacks and carpets, and the fibre is also used in many industrial sectors, e.g. to make dashboards in vehicles (Kimaro et al., 1994). It is the world's sixth most important fibre crop, representing 2% of the global production of plant fibres and accounting for about 70% of the world's hard fibres (FAO 2012). The world largest producers are Brazil, Tanzania, Kenya and Madagascar (FAO, 2012).

In Kenya, sisal was first introduced in 1903, and today, large-scale sisal plantations are found in the ASALs (constituting about 80% of the land in the country), with the lowland part of Taita Taveta County in southern Kenya producing most of the sisal (Githire, 1987). The vast area under sisal estates makes them an important land-use type in the region. However, whether the sisal estates are an important contributor to agricultural GHG emissions at the regional scale remains unclear. The recent ban on plastic bags in Kenya has increased the demand for sisal products, because sisal could provide more environmental friendly alternative to plastic (Njagi, 2018). Based on this and the fact that sisal, as a CAM plant, is well adapted to the current climate, there is a likelihood that the area under sisal will expand in the future.

Therefore, the aim of the present study was to advance our understanding of F_S from sisal plantations in southern Kenya. Our specific objectives were: 1) to assess the effects of sisal stand age on F_S and how they compare to bushland, representing the natural surrounding land cover type; 2) to investigate temporal variations in F_S within and across each sisal stand age and bushland; and 3) to explore the major environmental drivers of both temporal and spatial variations in F_S, including soil moisture, soil temperature, vegetation cover, soil properties and management activities. We hypothesized that F_S varies as a function of sisal stand age owing to the differences in root respiration. The second hypothesis was that F_S would vary across the different seasons, and more specifically, that F_S would be higher in wet than in dry seasons. The third hypothesis was that F_S would be primarily dependent on soil moisture and vegetation cover, which differ with the season and stand age, but less dependent on temperature due to its marginal intra-annual variation in the tropics.

2. Methodology

2.1. Site information

Teita Sisal Estate (3°30′S, 38°24′E; average elevation of 844 m above sea level (a.s.l.)), covers an area of 129.5 km^2 next to Mwatate town in the lowlands of Taita Taveta County, Southern Kenya (Fig. 1). With its cultivated area of 88.5 km^2 (Mr Mrombo, personal communication on 19 May 2020) it is the largest sisal estate in East Africa and the third largest in the world (Tsuda, 2019) active in growing sisal fibre for manufacturers in textile and other industries. The study area has a semi-arid climate with two rainy seasons: a long rainy season between March and May with a peak in April, and short rainy season between October and December, with a peak in November (CIDP, 2014). In the long-term average, the long rainy season is longer and brings more precipitation compared to the short rainy season. January and February are usually hot and dry, while from June to September it is cold and dry (CIDP, 2014). The mean annual rainfall from long-term observations (1990–2018) at the Teita Sisal Estate is 612 mm. The mean annual air temperature is 25.2 °C, with a minimum mean monthly temperature of 20.6 °C in June and July and a maximum of 31.2 °C in March. The soils are rhodic ferralsols characterized by dark red, very deep, acid sandy clay soil. These soils are very old, highly weathered and thus characterized by low nutrient contents (CIDP, 2014).

At the Teita Sisal Estate, sisal is planted in blocks of different varieties and timings with access roads for management purposes (Fig. 2). The varieties include *Agave sisalana, Agave hildana and Agave hybrid 11648*, with the latter as the main variety in most of the blocks in the estate (Mr Mrombo, personal communication on 19 January 2019). This is because it produces more leaves during its life cycle and is more resistant to drought compared to the other two varieties (Kimaro et al., 1994).

During the planting of new sisal, the land is prepared in advance, which includes vegetation clearance, removal of stones and rubble, and ploughing. The young plants propagated from bulbils or rhizomes of mature plants are kept in nurseries for about 12 to 18 months. These are then transplanted to the field at the onset of the rainy season. In the field, sisal is planted in double rows spaced 2–3 m apart with a plant population of about 5000 sisal plants per hectare. Mostly, about 40 t ha^{-1} of sisal waste is applied as fertilizer at the time of planting. Herbicides are also applied once after sisal planting to control common weeds, including couch grass (*Cynodon dactylon*), nut grass (*Cyperus rotundus*), African couch (*Digitaria abyssinica*), Lalang (*Imperata cylindrica*) and Guinea grass (*Megathyrsus maximus*) (DAFF, 2015). Management for subsequent years includes destumping, desuckering, bush clearing and mowing. Adjacent to the sisal plantation in the east, south and west, and on a hill (up to 1170 m a.s.l.) within the sisal estate, is bushland, characterized by thorny shrubs and small trees, mainly *Acacia* spp. and *Commiphora* spp. (Pellikka et al., 2018). The shrubs vary in height from 2–5 m, while the field layer consists of herbs and annual or short-lived perennial grasses less than 1 m tall. Grazing by wildlife (such as elephants, gazelles, giraffes and zebras) and livestock (cattle and goats) occurs in both the bushland and the sisal plantations.

2.2. Experimental design

For consistency, we chose sisal stands with the same sisal variety (*Agave hybrid 11648*), climate and topography (slope <10%) as our study sites. Additionally, the stands had been under similar management practices since their establishment. Considering the life span of 8 to 14 years of the *Agave hybrid 11648* variety (Kimaro et al., 1994), we selected seven sites with sisal stands of different ages (young: 1–3 years;

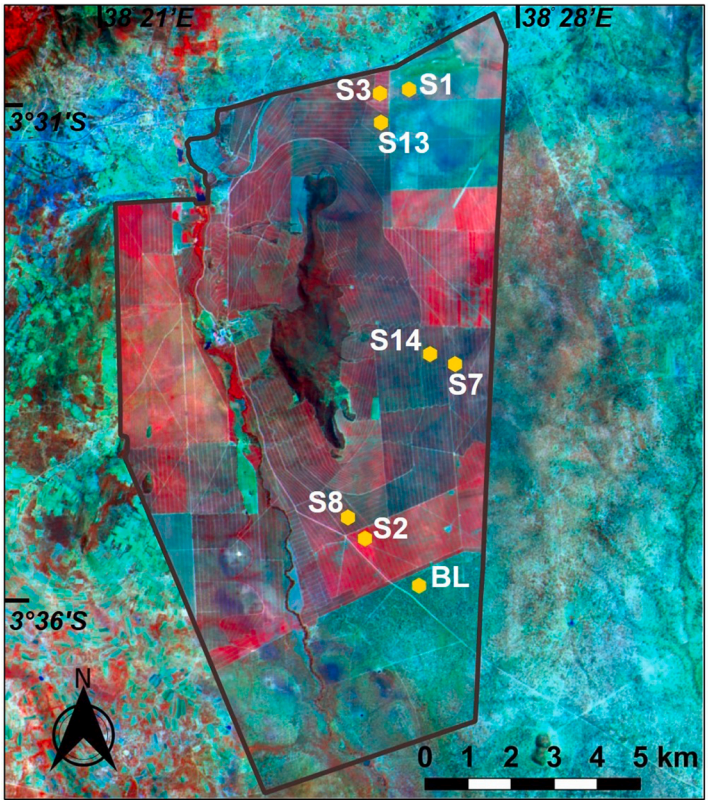

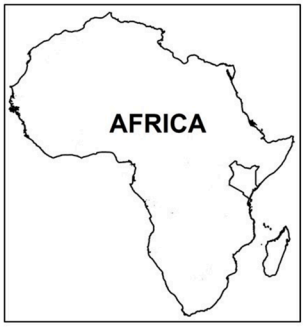

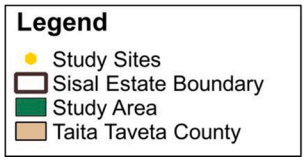

Fig. 1. Teita Sisal Estate in Taita–Taveta County, southern Kenya, showing the eight study sites depicted on a false-colour composition of a Sentinel-2A satellite image, 16 April 2019, from the Sentinels Scientific Data HubCE4 (ESA, 2015). Vegetation appears in different shades of red based on the types and condition, bare soils and developed areas as various shades of cyan and green. Boundaries were acquired from World Resources Institute (retrieved from https://www.wri.org/resources/data-sets/kenya-gis-data, last access 23 February 2020).

Fig. 2. Sisal stands at Teita Sisal Estate with ages of (a) one year in S1, (b) 7 years in S7 and (c) 13 years in S13, and (d) bushland adjacent to the sisal plantation.

mature: 7–8 years; old: 13–14 years) (see Table 1). The sites are referred to in this study using the prefix S for stand followed by the age in years (S1, S2, S3, S7, S8, S13 and S14). For comparison with surrounding land use types, a control site was established adjacent to the sisal plantation in the bushland (BL), which is reserved for conservation by the estate.

At each of the study sites, three random plots were selected for GHG measurements. In each of these plots, we installed three PVC chamber collars (27 cm × 37.2 cm × 10 cm), which were inserted about 5–8 cm

into the soil (see Pelster et al., 2017) for more details of the GHG chambers; for the technique, we refer to Hutchinson and Mosier, 1981; Rochette, 2011). Proximity to plot edges and main or feeder roads was avoided to eliminate edge effects and disturbance. These collars remained in the field for the entire study period to minimise soil disturbance (Søe et al., 2004). Soil GHG measurements were scheduled once per week from 17 January to 4 December 2019 at all eight study sites.

2.3. Data collection and processing

2.3.1. Soil GHG measurements

Soil GHG measurements using the static chamber method and a subsequent analysis by gas chromatography (GC, model SRI 8610C) followed the same procedure as described in Wachiye et al. (2020). In brief, it involved fitting a grey opaque lid (27 cm × 37.2 cm × 12 cm) covered by reflective tape on each chamber collar. Four gas samples were then collected from the chamber headspace every 10 min (time 0, 10, 20, 30 min) after lid deployment (Rochette, 2011) using a propylene syringe (60 mL). The gas pooling method proposed by Arias-Navarro et al. (2013) was adopted, where 20 mL of headspace air was collected from each of the three chambers in each plot, resulting into a 60-mL composite gas sample. The glass vials were flushed of any gases using the first 40 mL of the sample, while the remaining 20 mL was transferred into the 10 mL vial and overpressure was created to reduce contamination of the gas with ambient air during transportation (Rochette and Bertrand, 2003). The change in air temperature within the chamber headspace was monitored using a digital thermometer. Gas samples were analysed at the Mazingira Centre, International Livestock Research Institute (see mazingira.ilri.org) using gas chromatography (GC; model SRI 8610C). The GHG concentrations in each vial were determined by assessing the peak area of the gas samples in relation to the peak areas of standard gases using a linear model for CO_2 and CH_4, while a power regression was used to assess N_2O concentrations. We adopted a consistent quality control check to remove possible outliers that might have been a result of chamber leakage, vial mix-up or GC malfunction by evaluating the change in CO_2 concentrations over 30 minutes (for the four data points). Typically, CO_2 has a more robust and continuous flux than CH_4 and N_2O (Collier et al., 2014). Hence, CO_2 concentration data points were filtered by using the goodness of fit. This was done by calculating the normalized root mean square error (NRMSE) (see Christiansen et al., 2011) for each fit. The NRMSE is the root mean square error (RMSE) divided by the range of CO_2 concentration during the deployment time. Thus, a low NRMSE meant low headspace disturbance (Christiansen et al., 2011). Therefore, data points with a NRMSE ≤ 0.2 and coefficient of determination $R^2 > 0.9$ were included in further analyses. Furthermore, data points that exhibited a decline in the CO_2 concentration over time were presumed to indicate leakage and were discarded. This is because our chambers were opaque and thus photosynthesis was inactive during the chamber deployment time. Nonetheless, negative N_2O and CH_4 fluxes were accepted, as uptake of a particular gas by the soil can occur (Chapuis-Lardy et al., 2007; Topp and Pattey, 1997). F_S were calculated using Eq. (1).

$$F_S = \frac{(\Delta c/\Delta t) \times V_{ch} \times M_w}{A_{ch} \times M_v} 60 \times 10^6 \quad (1)$$

where F_S is the soil GHG flux (CO_2, N_2O, or CH_4), $\Delta c/\Delta t$ is the change in the chamber headspace gas concentration over time (i.e. slope of the linear regression), V_{ch} is the volume of the chamber headspace (m^3), M_w is the molar weight (g mol^{-1}) of C for CO_2 and CH_4 (12) or N for N_2O (2 x N = 28), A_{ch} is the area covered by the chamber (m^2) and M_v is the pressure- and temperature-corrected molar volume (see detail in Brümmer et al., 2008). The 60 and 10^6 are constants used to convert minutes into hours and grams to micrograms, respectively. Fluxes are expressed as mg C m^{-2} h^{-1} for CO_2 and CH_4, and μg N m^{-2} h^{-1} for N_2O. We calculated the minimum limit of detection (LOD) for each gas according to Parkin et al. (2012). However, all data were included in the analysis, including those that fell below the LOD, to provide an insight into the distinct measurements and clarifications on the set of environmental observations in line with Croghan and Egeghy. (2003).

2.3.2. Meteorological data

Alongside each gas sampling, volumetric soil water content (W_S, %) and soil temperature (T_S, °C) were measured at a depth of 5 cm adjacent to the flux chambers using a handheld data logger with a GS3 sensor (ProCheck, METER Group Inc., USA). Air temperature and atmospheric pressure were recorded using a handheld digital thermometer and Garmin GPSMap 64. A weather station was installed at S7, where air temperature (°C) was measured using a digital thermometer and rainfall (mm) using a tipping bucket rain gauge (ARG100, Campbell Scientific, USA) connected to a CR200X data logger (Campbell Scientific, USA). Rainfall data revealed a delay in the onset of the long rains (referred in this study as the long wet season (LWS)), which started in the first week of April instead of the second week of March (see Fig. S1 in supplementary) and in June. The short rains (also the short wet season (SWS)) occurred from October until the end of the year 2019. The onset of the wet season was defined as the first wet day of a three-day wet spell receiving at least 20 mm and without a more than ten-day dry spell (<1 mm) for the next 20 days after 1 March and 1 September for the long and short rains, respectively (Marteau et al., 2011). The end of the wet seasons was defined as the first of ten consecutive days without rain. Thus, the short dry season (SDS) were observed from January to end of March and the long dry season (LDS) from end of June to the end of September 2019.

2.3.3. Vegetation characteristics

Sisal is an evergreen perennial crop that retains foliage throughout the year. Due to harvesting and other management interventions in stands of different ages, we expected this to affect the sisal cover in each of these stands, which would eventually affect F_S. In addition, the understorey vegetation, such as grasses and weeds, has a pronounced seasonal cycle compared to sisal plants, which can influence seasonal variations in F_S. For seasonal variation of the understory vegetation, which also included the sisal plant, we acquired Enhanced Vegetation Index (EVI) data from Terra Moderate Resolution Imaging Spectroradiometer (MODIS) from 1 January 2019 to 19 December 2019. The MODIS EVI Level 3 (MOD13Q1) products data are generated at 16-day intervals with a spatial resolution of 250 m (Didan et al., 2015; https://ladsweb.modaps.eosdis.nasa.gov). We therefore acquired EVI data that matched or were close to our sampling dates, resulting in 22 EVI images. The pixels were then geographically subset using the latitude and longitude of each study sites and reprojected to WGS84 projection. The EVI computes vegetation greenness using Eq. (2) (for details see Huete et al., 1997), which can be used as a proxy for photosynthetic activity. EVI is designed to reduce the effects of atmospheric and canopy background thus optimising the green vegetation signal making it more sensitive at higher green biomass levels (Huete et al., 1997).

$$EVI = G \frac{\rho_{NIR} - \rho_{red}}{\rho_{NIR} + C_1 \times \rho_{red} - C_2 \times \rho_{blue} + L} \quad (2)$$

To assess the difference in the sisal cover in each stand, we estimated the dry leaf biomass (Mg ha^{-1}) in square-shaped plots (400 m^2 in area) next to the chamber sites using a locally developed allometric model for sisal leaves (Vuorinne et al., 2021a). The field survey was undertaken on 22 to 29 of August 2019. The plots were oriented with two sides parallel to the sisal rows such that four double rows (= 8 single rows) were inside the plot (see Fig. S4). The number of plants in the two midmost double rows was counted and multiplied by two to estimate the number of plants in the plot. The leaves were counted, and plant height and maximum leaf width were measured from one subjectively determined representative plant in the two midmost rows (Vuorinne et al., 2021b).

Plant height was measured with a measurement tape from topsoil to the terminal spine of the leaf unfolding upwards from the middle of the rosette. Maximum leaf width was measured with a measurement tape along the upper surface of the leaf. The mean values of these two plants were calculated to constitute representative plot-specific plant metrics. The number of leaves was multiplied by the number plants to obtain the total leaf count per plot. An allometric model (Eq. 3) was then used to predict the biomass (*B, grams*) of a representative leaf as:

$$\log(B) = -4.12 + 0.84 \log(W^2H) \quad (3)$$

Where W is the maximum width of the leaf (cm) and H is the height of the plant (cm) (Vuorinne et al., 2021a). Predicted values were transformed back to the original scale with Baskerville's (1974) logarithmic bias correction factor (*CF*) added to the predicted values using Eq. 4:

$$CF = (SE/2)^2 \quad (4)$$

Where *SE* is the standard error of the mean. Finally, stand-level biomass (Mg ha^{-1}) was estimated by multiplying the mass of the leaf by the total number of the leaves in the plot and by normalizing the product by the plot area.

2.3.4. Soil properties

Soil samples to determine soil organic carbon (SOC), total nitrogen (TN), soil texture, pH and bulk density were collected twice during this study. Nine randomly selected points at each site were sampled at a depth of 0–20 cm using a soil auger and soil bulk density ring of known volume (Eijkelkamp Agrisearch Equipment, Giesbeek, The Netherlands). Soil samples were stored in airtight polyethylene bags, labelled accordingly and transported in cooler boxes to the Mazingira Centre for analysis within 48 hours. In the laboratory, samples were stored at 4 °C until processing within 14 days. Soil water content and bulk density were determined by drying soil samples collected with bulk density rings of known volume at 105 °C for 48 h. A subsample of field moist soil was air-dried and sieved (to <2 mm) for pH and texture analysis. To assess the SOC and TN content, a duplicate of 20 g of fresh sample was oven-dried at 50 °C for 48 h and ground into a fine powder (<0.25 mm) using a ball mill (Retsch ball mill, Haan, Germany) and analysed using an elemental analyser (Vario MAX Cube Analyzer Version 05.03.2013). Soil texture was determined using the hydrometer technique (Scrimgeour, 2008; Reeuwijk, 2002). Soil pH was measured in a soil: distilled water suspension (1:2.5) using a pH meter (3540 pH and conductivity Meter, Bibby Scientific Ltd, UK). Ammonium (μg NH_4^+-N g^{-1} DW) and nitrate (μg NO_3^--N g^{-1} DW) were extracted from 8 g of fresh sieved soil with 40 mL of 1M potassium chloride (KCl), which was shaken for 60 minutes (Edmund Buhler GmbH SM-30 Lateral Shaker) at room temperature. The samples were then filtered (Whatman filter paper No. 42) and frozen at -18 °C until analysis. Analysis was then performed using colorimetric assays on a photometric microplate reader (EPOCH, BioTek) (Hood-Nowotny et al., 2010).

2.4. Statistical analysis

Daily, monthly and seasonal means of F_S were calculated for the entire study period based on mean hourly F_S estimated from the nine replicate flux chambers at each site. We used boxplots to display the overall difference in F_S between the sites and the temporal variability of F_S, W_S and T_S between sites across the study period. The boxplots display the minimum, first quartile (Q1), median, third quartile (Q3), and maximum of data distribution. We performed the Friedman test (a non-parametric test comparable to a repeated measures ANOVA) to assess whether the effects of (i) stand age and bushland, (ii) months or seasons (wet and dry seasons) on F_S were significant given that the data were not normally distributed even after transformation (log and square-root). Months or season were treated as a blocking factor in the analyses. A *post hoc* comparison using Wilcoxon signed-rank tests was conducted with a Bonferroni correction applied, when significant differences existed. Using the same tests, the differences in T_S and W_S in relation to the stand age and across the study period were assessed. The relationship between F_S and T_S and/or W_S within each study site was then evaluated using both linear and nonlinear regressions and their combination shown in Table 2, and using R^2, residuals, AIC and RMSE to choose the best-fit equations.

Cumulative annual F_S for each site were calculated by trapezoidal integration of daily fluxes with time. Therefore, relationships between cumulative F_S and the other environmental variables that were not measured daily, including soil pH, bulk density (BD), soil texture, SOC, TN, NH_4^+, NO_3^-, and aboveground leaf biomass and mean EVI, were evaluated as follows: Significant driver variables were identified by first applying Spearman correlation coefficients. Then, multicollinearity between the driver variables was tested using the variance inflation factor (VIF), and values with a VIF between 1–5 were accepted as not co-correlated and not requiring correction (Wanyama et al., 2019). Variables that were significantly correlated with fluxes and not co-correlated were then included in a stepwise multiple regression analysis, starting with variables with the highest correlation coefficients and with those that have been shown in other studies to be important in explaining F_S. All statistical tests were performed at the 5% level of significance. All statistical analyses and plotting were carried out using R 3.5.2 (R Core Team 2018), and summary values were expressed as the mean value ± standard error of the mean (SE).

3. Results

3.1. Soil GHG fluxes in a sisal plantation chronosequence

3.1.1. Soil CO_2 fluxes

Soil CO_2 flux rates measured from all sites ranged between 10 and 225 mg C m^{-2} h^{-1} (about 0.1 to 1.5 μmoles C m^{-2} h^{-1}) during the study period. The Friedman test revealed a statistically significant difference in CO_2 fluxes between stands of different ages (chi-squared = 23.1, df = 7, p = 0.002). In the sisal plantation, soil CO_2 fluxes increased with stand age from S1 to S3, dropped in S7 and S8 and increased again in S13 and S14 indicating a non-linear increase in CO_2 fluxes with stand age (Fig. 3a). The highest soil CO_2 fluxes on average were observed from the S14 (56 ± 4 mg C m^{-2} h^{-1}) and S3 (55 ± 5 mg C m^{-2} h^{-1}), and the lowest from S8 (38 ± 2 mg C m^{-2} h^{-1}). Significant differences were observed between S1 and S3, S13 and S14 ($p < 0.05$) and between stand S2 and S3 and S14. However, no differences in CO_2 fluxes ($p < 0.05$) were observed between S7 and S8, or between these two stands (S7 and S8) and the rest of the stands. CO_2 fluxes were higher (13–28%, $p < 0.05$) in all sisal stands than the observations from the adjacent bushland (BL) control site (that showed overall lowest observations: 32 ± 5 mg C m^{-2} h^{-1}) across the study period except in the month of November, where BL recorded the highest soil CO_2 fluxes.

Soil CO_2 fluxes from all sites displayed a similar bimodal pattern (Fig. 4a), which followed the dynamics of soil moisture (Fig. 4e). There was significant differences ($p < 0.05$) in soil CO_2 fluxes between the months and seasons. Soil CO_2 fluxes observed during both wet seasons ranged between 53 and 225 mg C m^{-2} h^{-1}, and were approximately 30%

Table 1
Studied sisal stand characteristics, Teita Sisal Estate, Kenya

Stand	Block	Year planted	Age (years)	Times harvested	Area (ha)
S1	9	2018	1	0	364
S2	3	2017	2	0	611
S3	4A	2016	3	1	235
S7	1T/H	2012	7	7	278
S8	1A	2011	8	6	316
S13	6B	2006	13	9	535
S14	6A	2005	14	9	378

Table 2
Regressions fitted to the soil climate dependence of soil respiration

Predictors	Regression	Equation
Soil temperature (T_S)	Linear	$F_S = a + b\ T_s$
	Exponential	$F_S = a\ exp^{b\ T_s}$
	Gaussian	$F_S = a\ exp^{b\ T_s + c\ T_s^2}$
Soil water content (W_S)	Linear	$F_S = a + b\ W_s$
	Power	$F_S = a\ W_s^b$
	Quadratic	$F_S = a + b\ W_s + c\ W_s^2$
Combined (T_S and W_S)	Gaussian + Quadratic	$Fs = exp^{a\ T_s + b\ T_s^2} + (c\ W_s + d\ W_s^2)$

F_S denotes soil CO_2 flux (mg C m^{-2} h^{-1}) and N_2O flux (μg N m^{-2} h^{-1})
T_S is soil temperature and W_S is soil moisture, both measured at a depth of 5 cm
a, b, c, d and *e* are the corresponding fitted parameters for each model

higher than fluxes observed during the two dry seasons (Fig. 5a). During the short dry season (between January to end of March), CO_2 fluxes were very low (below 29 ± 5 mg C m^{-2} h^{-1}) at all the sites and rapidly increased in early April, which coincided with the onset of the long rainy season. This was followed by a decline in soil CO_2 fluxes from mid-June, the end of the long rainy season. Soil CO_2 fluxes remained low throughout the long dry season until September and recording the lowest overall soil CO_2 fluxes during the year, but increased rapidly at the beginning of the short rainy season in October to December 2019. Maximum soil CO_2 fluxes were observed in October to December (ranging from 59 to 225 mg C m^{-2} h^{-1}). The pattern of higher fluxes in the older stands was very clear during the wet seasons. In the dry seasons, CO_2 fluxes increased from S1 to S3, but the mature (S7 and S8) and older stands (S13 and S14) displayed varying soil CO_2 fluxes with no distinct trend (see SDS and LDS in Fig. 4a).

3.1.2. Soil N_2O fluxes

Soil N_2O fluxes were very low throughout the study year, ranging between -7.7 and 17 μg N m^{-2} h^{-1} at all the sites. The Friedman test revealed a statistically significant difference in N_2O fluxes between stands of different ages ($p < 0.05$). In detail, no significant difference in N_2O fluxes was observed between S1 and S7, but both S1 and S7 were significantly different from all the other sites except sites S2 and S3 ($p = 0.02$) (Fig. 3b). In addition, N_2O fluxes from all the sisal stands were not significantly different ($p > 0.05$) from those observed in the bushland. During the year of observations, N_2O fluxes varied without following the same strong seasonal pattern (Fig. 4b) as observed for the CO_2 fluxes (Fig. 4a). Nonetheless, season had an effect on N_2O fluxes ($p < 0.05$) and the measurements revealed a slight increase in N_2O fluxes at the onset of both wet seasons across all sites. However, this effect was only significant for the short rainy season ($p < 0.05$). Combining both wet seasons, N_2O fluxes were 37% higher than during the dry seasons (Fig. 5b). About 34% of all measured N_2O flux rates were negative during the study period, mostly in the dry seasons. This is an indication of an uptake of N_2O during parts of the year and at all the sites.

3.1.3. Soil CH_4 fluxes

Daily soil CH_4 fluxes, including those from bushland, ranged between -0.4 and 1.9 mg C m^{-2} h^{-1}. However, the majority (about 89% of 1068 CH_4 flux data points from all sites) of these values fell below the limit of detection (LOD; ±0.02 mg C m^{-2} h^{-1}). Moreover, the values did not differ between sites (Fig. 3c). However, we noted that most of the positive CH_4 fluxes were observed at sites S3, S8, S13 and S14, while the mean CH_4 fluxes from the other stands and bushland was consistently negative. We did not observe any pronounced response to the onset of the wet season as occurred for CO_2 and N_2O fluxes (Fig. 4c,Fig. 5c).

3.2. Effect of soil water content and soil temperature to soil CO_2 efflux

Soil water content (W_S) showed a bimodal pattern following rainfall (Fig. 4e), where W_S was significantly higher in both wet seasons (ranging from 11% to 29%; $p < 0.05$) compared to the dry seasons (<10%) at all the sites. The temporal coefficient of variation (CV) in W_S ranged from 50% to 64% across all study sites. Spatial CV ranged between 7% and 53% across the year, with the highest spatial variation observed at the onset of the rainy season in April and October. However, on average W_S did not differ significantly ($p < 0.05$) between the sites. The results from regression analysis at each site indicated a significant positive relationship ($p < 0.05$) between CO_2 fluxes and W_S. Comparing the models that were applied, quadratic regression emerged as the best model (with the highest R^2 value and smallest AIC and RMSE) describing the relationship between the CO_2 flux and W_S both overall and at each site (Fig. 6). It explained between 24% and 52% of the variation in CO_2 fluxes (details of the other models is provided in the supplementary). On the other hand, overall mean N_2O fluxes did not show any relationship with W_S. Nonetheless, a significant effect of W_S on N_2O fluxes at sites S7, S14 and BL was observed, but the R^2 was very weak. Furthermore, we did not observe any correlation between CH_4 fluxes and W_S overall or within any of the site.

Variations in T_S, on the other hand were very small (Fig. 4d), with a temporal CVs ranging between 12% and 16% across all the study sites. Equally, the spatial CV across the year was low (between 7% and 15%). The maximum T_S was observed in February (35.2 ± 0.5 °C) and March (33.1 ± 0.5 °C) and the minimum in June (26.7 ± 0.3 °C) and August (27.4 ± 0.4 °C). Not surprisingly, the slight spatial T_S variance did not explain much of the variation in CO_2 fluxes, N_2O fluxes and CH_4 fluxes across sites and within each site. Thus, adding T_S as an explanatory variable to W_S did not improve the model. These results are provided in the appendix data (Table S.5).

3.3. Effect of vegetation on soil GHG fluxes

EVI differed between the seasons and the sites, and on average, the

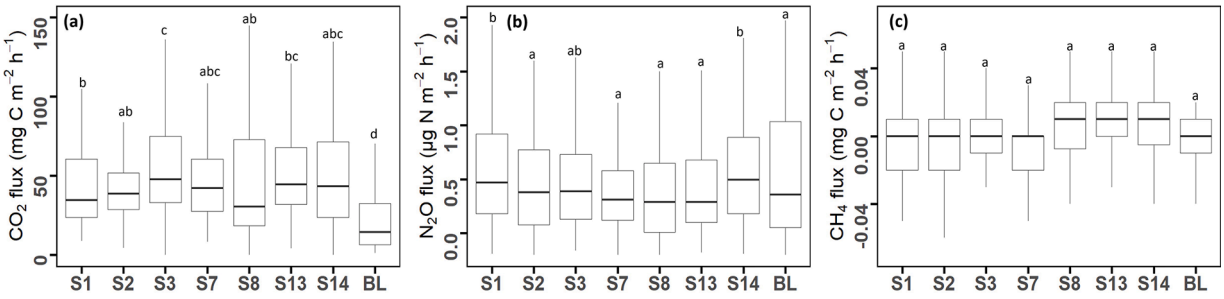

Fig. 3. Difference in (a) soil carbon dioxide, (b) soil nitrous oxide, and (c) soil methane fluxes measured between 17 January and 4 December 2019 at Teita Sisal Estate. S1-S14 are sisal stands of different ages (in years), BL is bushland. The boxplot display the minimum, first quartile (Q1), median, third quartile (Q3), and maximum of data distribution. The letters denote significant differences between the sites at p<0.05 (Wilcoxon signed-rank tests).

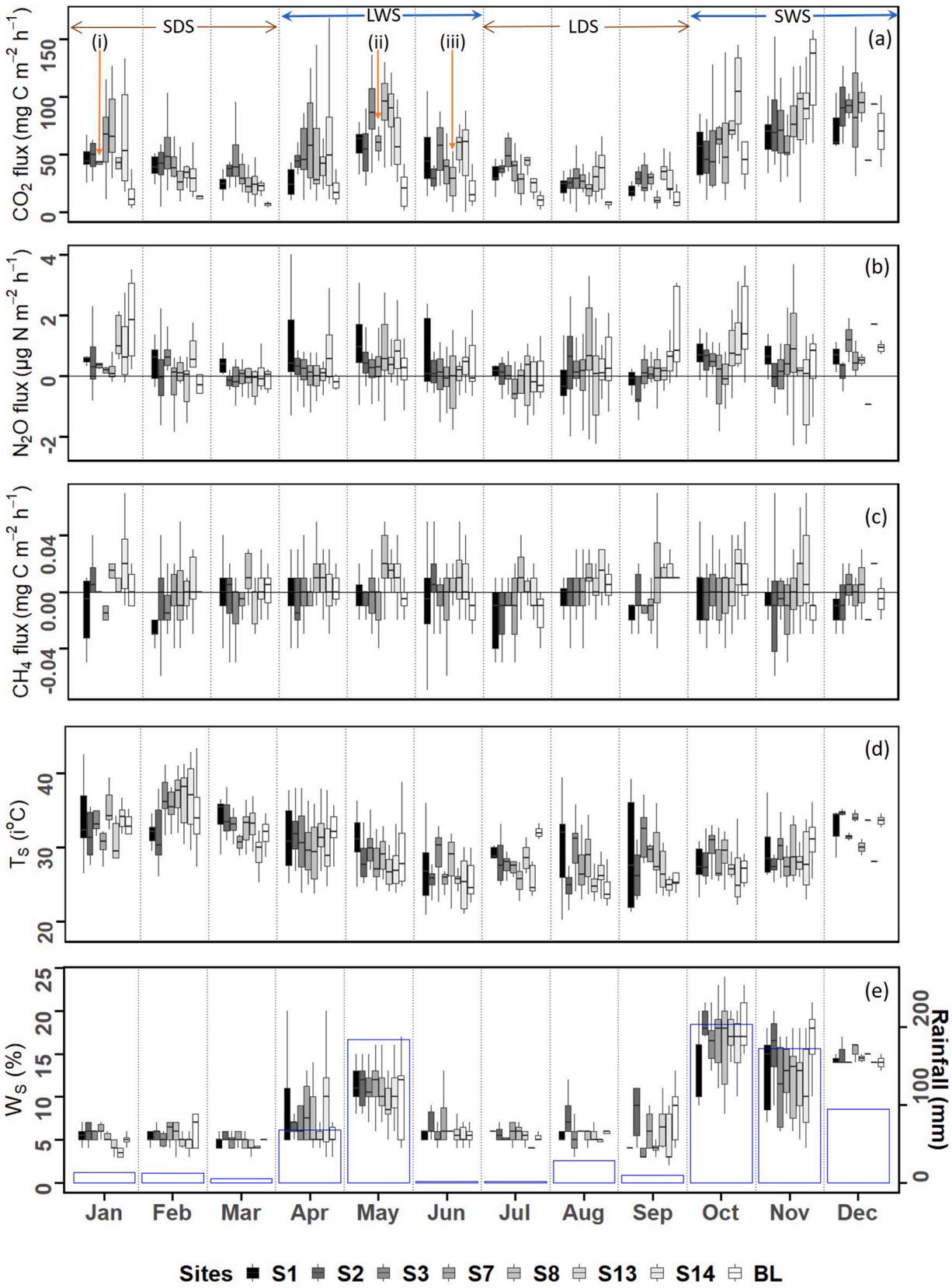

Fig. 4. Monthly soil (a) carbon dioxide, (b) nitrous oxide and (c) methane fluxes, and (d) soil temperature (T_S) and (e) percentage soil water content (W_S) with the blue bars showing total monthly rainfall measured between 17 January and 4 December 2019 at Teita Sisal Estate at S7. S1-S14 are sisal stands of different ages (in years), BL is bushland. The orange arrows indicate timing for (i) weeding in S3, (ii) harvesting and desuckering in S7 and (iii) cutting of grass in S8. LWS and SWS denote the long and short wet season, respectively, while SDS and LDS denotes short and long dry season, respectively.

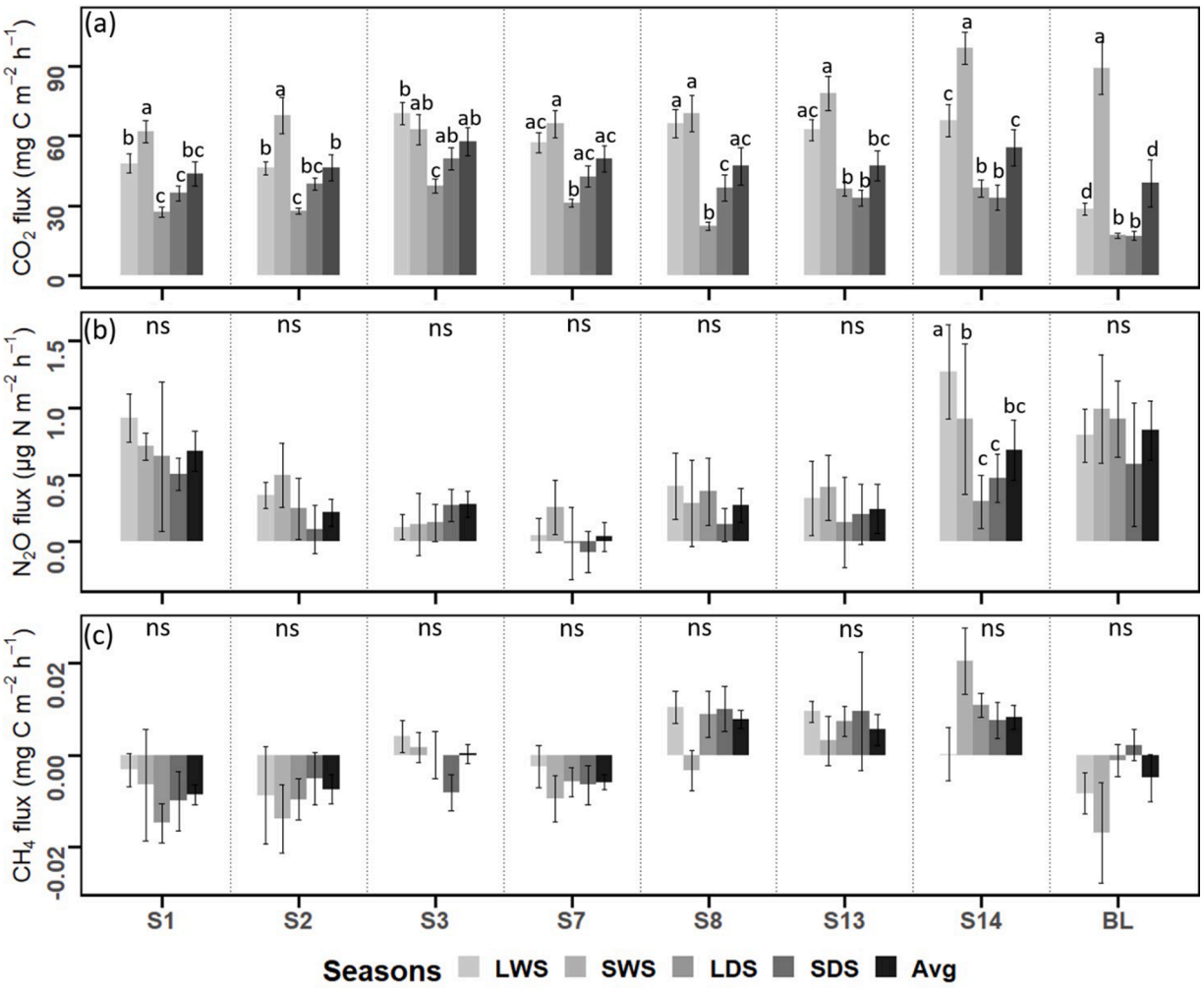

Fig. 5. Seasonal differences in mean (a) CO_2, (b) N_2O, and (c) CH_4 fluxes between the long wet season (LWS) and short wet season (SWS), the long dry season (LDS) and short dry season (SDS), and the annual (Avg) mean fluxes for all the study sites. Note that the limit of detection for CH_4 is ±0.02 mg C m^{-2} h^{-1}. Letters denotes significant difference at $p<0.05$ and "ns" not significant (Wilcoxon signed-rank tests).

mean EVI was the highest in S14 (0.45 ± 0.02), and the lowest in S1 (0.27 ± 0.02) and at the bushland (BL) control site (0.30 ± 0.04). At each sites, we found that monthly EVI was highly seasonal with the highest EVI values observed during the two wet seasons when vegetation was green, while the lowest EVI during the two dry seasons (Fig. 7), which coincided with the drying of most grasses as affected by these annual fluctuations in water availability (Ludwig et al. 2001). We fitted a linear regression model between EVI and CO_2 and N_2O fluxes, and the results indicated a moderate to strong relationship between EVI and CO_2 fluxes ranging from 18% to 73% (Fig. 8). Nevertheless, EVI values were not correlated with soil N_2O fluxes at any of the sites. However, overall cumulative soil N_2O fluxes were negatively correlated with the annual mean EVI ($R = 0.19$; $p = 0.03$).

Sisal dry leaf biomass was assessed once during the study period (late August), and the highest dry leaf biomass was observed in S2 (27.08 Mg ha^{-1}), followed in declining order by S14 (14.3 Mg ha^{-1}), S8 (11.2 Mg ha^{-1}), S3 (11.1 Mg ha^{-1}), S13 (10.9 Mg ha^{-1}), S7 (4.3 Mg ha^{-1}) and S1 (4.2 Mg ha^{-1}). Site S7 had just been harvested in May, three months before the biomass assessment. Regression analysis revealed a positive relationship between the cumulative annual CO_2 fluxes and the leaf dry biomass ($R^2 = 0.83$; $p = 0.04$) but no significant relationship ($p > 0.05$) with N_2O fluxes was observed.

3.4. Effect of soil and stand properties on soil GHG fluxes

We found a slightly higher clay content (%) in S8 (35.6 ± 0.9) and BL (31.6 ± 0.9) compared to all other sites. A similar pattern was observed for silt. In contrast, the sand content was the lowest in S8 (52.5 ± 0.6) and the highest in S14 (75.8 ± 0.5). Soil pH was the lowest in S3 (5.5 ± 0.1) and the highest in S2 (7.9 ± 0.1). NH_4^+ and NO_3^- were significantly higher in S1 than the other sites, while NH_4^+ was the lowest in S13 and NO_3^- was the lowest in S8. SOC, TN and BD did not differ among sites in the sisal plantation and bushland ($p > 0.05$), and therefore, for all gases and at all sites, stepwise multiple regression yielded only one significant driving factor ($p < 0.01$), where cumulative soil N_2O fluxes were positively correlated with TN ($R = 0.71$; $p = 0.01$).

4. Discussion

4.1. Soil CO_2 fluxes

Overall, soil CO_2 flux rates measured during study period ranged between 10 and 225 mg C m^{-2} h^{-1} (about 0.1 and 1.5 µmoles C m^{-2} h^{-1}) from all the sites. This is low compared to similar studies in plantations from other ecosystem (Smith et al., 2012; Wang et al., 2013; Wiseman and Seiler, 2004; Zhao et al., 2016). However, the results are within the range reported from other land use types in tropical savannah ecosystem similar to our study (Ardö et al., 2008; Livesley et al., 2011; Wachiye

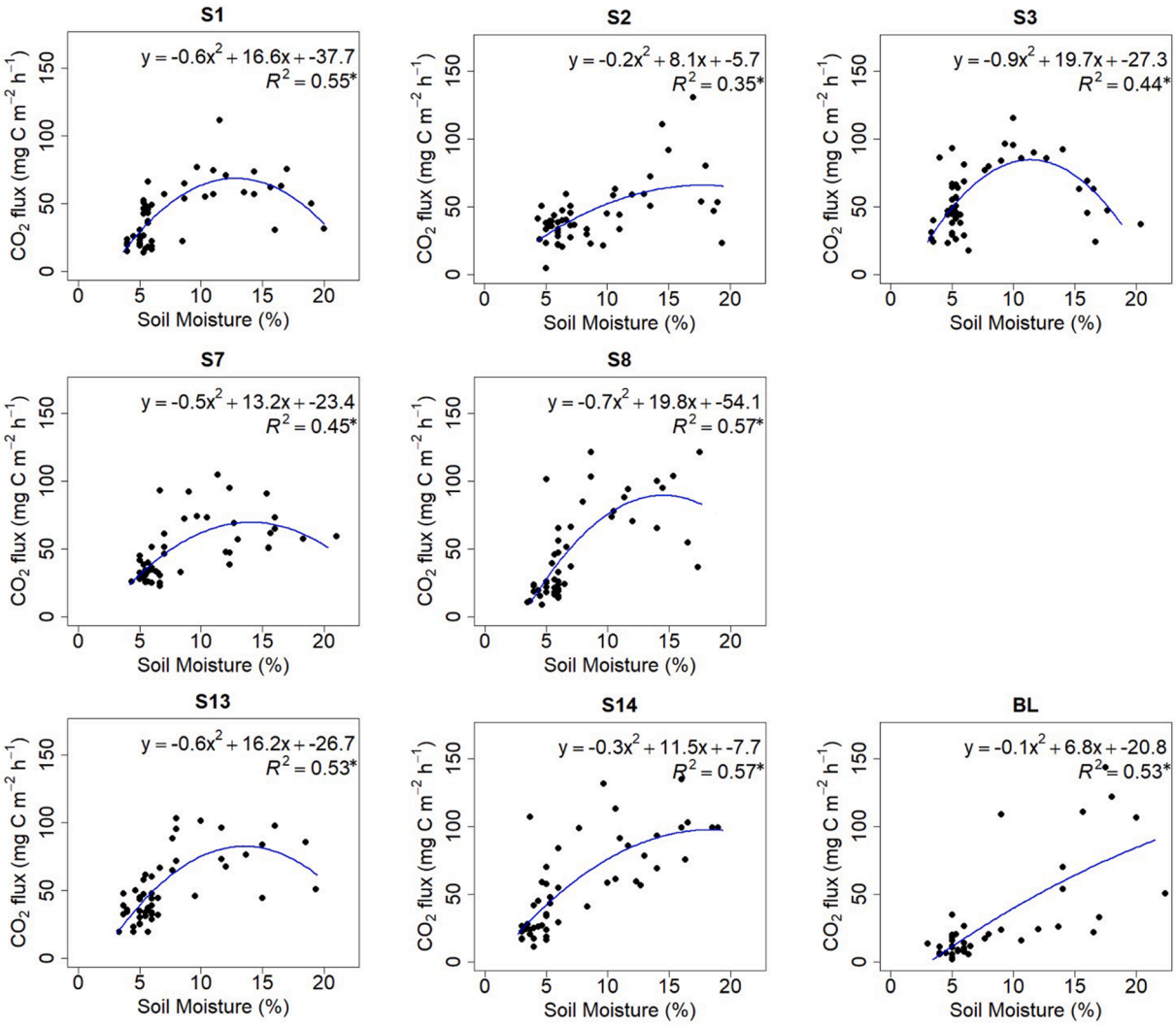

Fig. 6. Quadratic relationship between soil CO_2 fluxes and volumetric soil moisture in each study site from14 January to 3 December 2019. The coefficient of determination (R^2) is provided for each site with (*) representing significance at $p < 0.05$. S1-S14 are sisal stands of different ages (in years), BL is bushland.

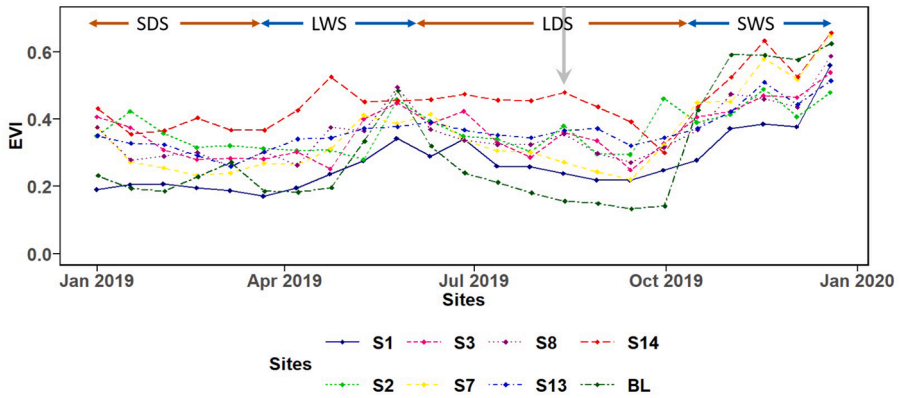

Fig. 7. Seasonal variation in Enhanced Vegetation Index (EVI) from 1 January to 29 December 2019 at each study site. The grey arrow shows the date for biomass assessment.

et al., 2020). Generally, low soil CO_2 flux can be attributed to low SOC content observed in savannah ecosystem when compared to tropical forest or temperate grasslands (Grace et al. 2006; Scholes et al., 1996).

Soil CO_2 fluxes first increased with stand age from S1 to S3, dropped in S7 and S8 and then increased again in S13 and S14. On average, the highest soil CO_2 fluxes were observed from stand S3 and S14 (56 ± 4 mg C m^{-2} h^{-1}), and the lowest from the mature stand in S8 (38 ± 2 mg C m^{-2} h^{-1}). Several studies reported an increase in CO_2 fluxes with stand age in oil palm and rubber plantations (Gao et al., 2019; Sigau and Hamid, 2018), as well as in forest plantations (Wiseman and Seiler, 2004; Yan

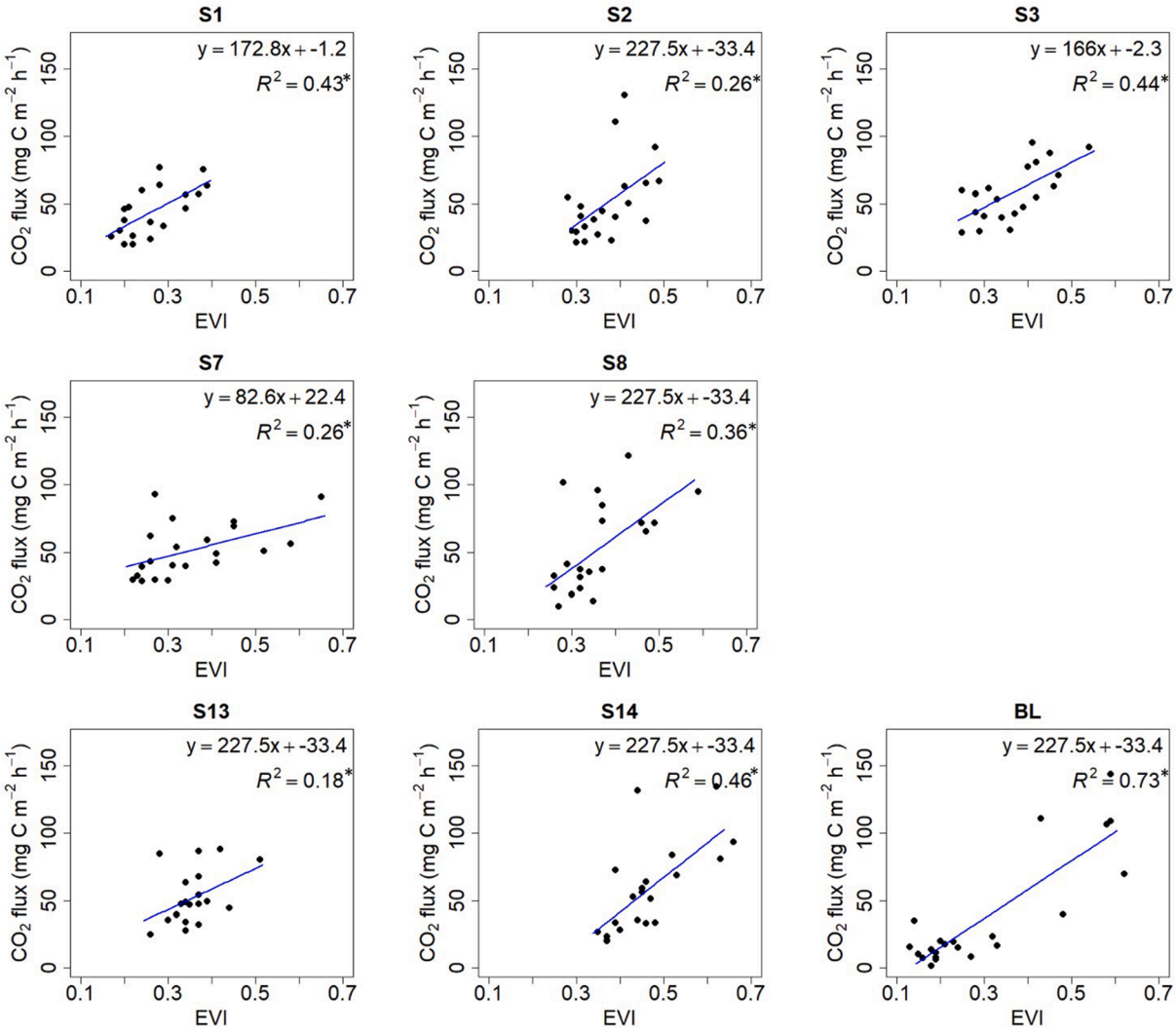

Fig. 8. Linear relationships between soil CO_2 fluxes and Enhanced Vegetation Index (EVI) in each study site from 14 January to 3 December 2019. The coefficient of determination (R^2) is provided for each site with (*) representing significance at $p < 0.05$. The sites are represented by S for stand followed by the age of the sisal stand

et al., 2011; Yin et al., 2016). The results were attributed to the effect of greater soil organic C and root activity in older than in younger stands. However, in this present study, the increase in CO_2 fluxes from S1 to S2 and S3 can also be attributed to an increase in the root network with stand age. This is an observation noted for all *Agave* plants, thus translating to greater root biomass and more root respiration (Nobel and Quero, 1986; Nobel et al., 1992). The drop in CO_2 fluxes in mature stands (S7 and S8), was probably an effect of harvesting, as these two stands were under active annual harvesting of sisal leaves for processing. After harvesting, only 25 leaves are left per plant (DAFF, 2015), which was reflected in the low annual dry leaf biomass for both stands S7 and S8 compared to the other sites. Apart from harvesting, desuckering in S7 in May and cutting of grass in S8 in June resulted in a considerable drop in CO_2 fluxes from these stands. A similar pattern was observed in July, August and September, months that were characterized by the removal of aboveground biomass. The decline in root respiration due to leaf area removal has been reported in several other studies (Bremer et al., 1998; Bingham and Stevenson, 1993). Harvesting of leaves reduces the photosynthetic activity of the plant, which in turn reduces root respiration as a result of decreased C substrate input into the soil (Bahn et al., 2009; Högberg et al., 2001).

Contrary to our study, other studies have reported a decrease in CO_2 fluxes with an increase in stand age of coniferous and deciduous trees in hemi-boreal forests in China and Ireland (Saiz et al., 2006; Zhao et al., 2016; Wang et al., 2002) and attributed it also to a decrease in root biomass with stand age. Yet others have observed a non-linear relationship in forests similar to this study (Law et al., 2003; Tang et al., 2006; Toland and Zak, 1994) but in these studies, CO_2 fluxes first increased with stand age, peaked at an intermediate age and subsequently declined with age. We can only speculate here that the differences between results from these studies and our results might be connected to differences in vegetation type (Raich and Tufekcioglu 2000), management activities (Grover et al., 2012; Högberg et al., 2001) such as the harvesting, and stand ages (Klopatek, 2002) found in these studies, as our study is the first from tropical sisal plantations.

Nevertheless, the CO_2 flux within a given stand is importantly influenced by the quantity of fine roots and the quality of soil carbon (C) pools (Klopatek, 2002). As our study design was developed to quantify GHG emissions, it was not feasible to assess root biomass. However, the fact that the soil organic C content, the substrate for soil microbial respiration (Zheng et al., 2009), did not vary between the stands observed suggests that root respiration represented the majority difference in CO_2 fluxes between our stands. Other reasons for differences in CO_2 fluxes with stand age could include the presence of other vegetation in our stands, such as grasses and weeds, especially in older stands. Weeding is mainly conducted in younger stands to control weeds, but in

older stands, grasses, weeds and other vegetation are allowed (DAFF, 2015).

Soil CO_2 fluxes were the highest in the wet season and the lowest in the dry season in relation W_S, showing a bimodal pattern at all sites. An increase in W_S in both the long and short wet seasons led to a rapid increase in CO_2 fluxes, an observation recorded at the start of both rainy seasons in April and October at all sites (Figs 4a and 5a), followed by a decline in CO_2 fluxes at the onset of the dry period (from mid-June). Soil W_S appeared to play a more significant role in explaining the variation of between 24% and 52% in CO_2 fluxes than T_S. An increase in W_S enhances root respiration due to the increase in active new plant and root growth, and possibly C allocation to rhizosymbionts, (Huxman et al. 2004; Kelting at al., 1998; Manzoni and Katul, 2014). Soil W_S also connects microorganisms with soluble substrates (Moyano et al., 2013), which can accumulate during the dry season and are then metabolized in the rainy season (Manzoni et al., 2012), thereby increasing microbial activity (Davidson and Janssens, 2006; Davidson, 2009; Grover et al., 2012) and thus soil CO_2 fluxes.

Soil T_S, on the other hand, displayed very narrow temporal and spatial variation across the study period, which might explain why T_S was less important in explaining the variation in CO_2 fluxes. This has also been reported in previous studies on tropical land use types (Castaldi et al., 2006; Grover et al., 2012; Livesley et al., 2011; Wachiye et al., 2020). The model with both W_S and T_S did not explain more variation in CO_2 fluxes than the model based on W_S, which may indicate that other factors may have also exerted strong effects on the seasonal variation in CO_2 fluxes in this study area. In the dry season, we documented a progressive reduction in CO_2 fluxes in relation to a decline observed in W_S (Figs 4a and 4e). The decline in W_S affects the diffusion of the organic carbon substrate and causes microbial stress and minimizes plant growth (Li et al., 2018), thus reducing CO_2 fluxes. The seasonality in CO_2 fluxes can thus be explained by the sisal plant rooting system, which shrinks in dry soil conditions to minimise water loss but quickly produces fine roots referred to as 'rain roots' after a rain event (Nobel and Sanderson, 1984). These rain roots generally desiccate as the soil subsequently dries, reducing their respiration rates to zero and causing irreversible damage (Nobel and Sanderson, 1984; Palta and Nobel, 1989). Additionally, sprouting and regrowth of grasses and new plants at the onset of the long and short wet seasons was evident at all sites, as reflected by an increase in EVI. Grasses are known to sprout more rapidly with the first rain event (Merbold et al., 2009), thus having a more pronounced seasonal variation across the year than sisal plants. The drying of the aboveground grasses and other plant tissues was also evident in the progressive reduction in EVI during this time. The results from linear regression analysis revealed a strong positive correlation between soil CO_2 fluxes with EVI ($p < 0.05$), explaining 16% to 78 % of the variation in CO_2 fluxes at all sites. The average CO_2 fluxes from the sisal stands in the wet season are within the same range (ranging from 50 to 200 mg C m^{-2} h^{-1}) as those observed in the croplands investigated by Rosenstock et al. (2016) and Wachiye et al. (2020). While CO_2 fluxes in bushland during this duration is within the range observed by Wachiye et al. (2020) in bushland.

We examined each season more closely to assess whether the pattern in CO_2 fluxes with stand age was consistent across the year. This is because in drier seasons, most of the understorey grasses and weeds dry up (as shown by a drop in the EVI in Fig. 7), reducing their contribution to root respiration. We noted that months in the wet season showed a clear increase in CO_2 fluxes with stand age. Nevertheless, in drier months (January, February, March, June and July), CO_2 fluxes first increased from S1 to S2 and S3, which we attributed to an increase in root network. A drop in S7 and S8 was observed, which was probably a result of harvesting as discussed before, followed by an increase in S13 and S14.

Overall, our control site (BL) represented the natural land-use type in the lowlands and showed the lowest CO_2 fluxes compared to all the sisal stands. Management activities in the sisal plantation, such as tillage, weeding and the use of fertilizer, may speed up the rate of decomposition of debris, litter and soil organic matter, thus increasing CO_2 fluxes (Boeckx et al., 2011) compared to BL, which is only under grazing and browsing from wildlife and livestock from nearby ranches. In addition, bushland recorded the lowest overall mean EVI, an indication that, on average, it had the lowest photosynthetic vegetation cover throughout the study period.

In bushland, during the dry season *Commiphora africana, C. campestris* and *C. lidensis* shed their leaves, and *Acacia* ssp. most of the leaves (Otieno et al., 2005) and grasses dried up almost completely, as depicted by the very low EVI observed during this time and hence affecting the annual mean CO_2 fluxes. The sisal plantation, on the other hand, had a relatively high annual mean EVI throughout the seasons as sisal is an evergreen perennial crop (Lüttge, 2004). The EVI values for September - October correlate well with biomass assessment of the sisal estate (Vuorinne, 2021b), in which the highest biomass was assessed using Sentinel data from September 29, 2019 for stands of 2 and 3 year of age, which also had the highest EVI values assessed in this study. These results are opposite to those reported by Wachiye et al., (2020), who observed higher soil CO_2 fluxes from bushland than cropland, and those of Brummer et al., (2009), who reported higher CO_2 fluxes in natural savannah than agricultural land. However, it needs to be stated that a sisal plantation is dissimilar in phenology from cropland and other agricultural landscapes as the plants and leaves are there throughout the seasons if they are not harvested. Thus, we attribute the differences found are due to the crop type cultivated. In the abovementioned studies, the crop types were generally annual species, with land preparation being annual and coupled with regular cultivation to remove weeds, affecting both root respiration and the soil C content (Raich et al., 2000). However, the sisal plant is perennial, with cultivation mainly carried out at planting, while herbicides are used to kill weeds instead of ploughing, and weeds are allowed to grow from 2 to 3 years after establishment (DAFF, 2015). These differences are bound to have an effect on soil CO_2 fluxes.

4.2. Soil N_2O fluxes

Soil N_2O fluxes observed from each study site throughout the year were very low (<5 μg N m^{-2} h^{-1}). The soil N content was similarly very low, with no variation between the sites, and thus could explain the low N_2O fluxes observed. This also can explain why we did not observe a significant differences among the stands in the sisal plantation and bushland. These results are comparable to other studies claiming that drier areas, such as in our study, exhibit low N availability due to very tight N cycling (Pinto et al., 2002; Grover et al., 2012). The role of N limitation as a factor in controlling N_2O fluxes has been stated by a number of studies (Castaldi et al., 2006; Grover et al., 2012). Therefore, the available N is mostly taken up by vegetation, leaving very little for denitrification (Castaldi et al., 2006). Furthermore, sisal plants require soil total nitrogen (TN) of more than 0.15% (Kimaro et at., 1994). However, all our stands had N contents ranging from 0.07% to 0.10%, which is well below the optimum amount required by sisal plants.

We could not detect a similar seasonal pattern of N_2O fluxes as observed for CO_2 fluxes. Soil N_2O fluxes were generally very low at all sites and did not change significantly with changes in the environmental conditions. Regression analysis demonstrated a significant effect of W_S on N_2O fluxes only at sites S7, S14 and BL, but the R^2 value was very low. The most likely explanation could also be due to the low N levels observed at all the sites, which may have overruled the potential of other factors controlling N_2O fluxes (Grover et al., 2012). This has also been observed in other studies (Livesley et al., 2011; Wachiye et al., 2020). We only noted a slight increase in N_2O fluxes at the onset of the long wet season at all sites. A likely explanation for this is that an increase in soil moisture availability increased soil microbial activity, thus facilitating the rapid breakdown of plant litter and increasing N availability (Davidson et al., 1998), which in turn led to an increase in N_2O fluxes.

Additionally, soil moisture increases the movement of substrates necessary for microbial growth and metabolism (Davidson et al., 2000). However, the reduction could be the result of increased competition for the available N by new and resprouting plants, and the increase in soil microbes thus increased competition for N (Bate, 1981) as reflected by a negative correlation with EVI. Several studies have also observed this pattern in similar environments in Africa and Australia (Castaldi et al., 2006; Livesley et al., 2011; Wachiye et al., 2020).

Soil N_2O fluxes from all the sites are in the same range (from -1.0 to 1.5 μg N m^{-2} h^{-1}) as observed in other studies in semi-arid environments (Grover et al., 2012; Livesley et al., 2011). Soil N_2O fluxes from all stand ages in the sisal plantations were slightly lower than 2.7 μg N m^{-2} h^{-1} observed from a cropland in the lowlands of Taita Taveta County by Wachiye et al., (2020). We attribute this dissimilarity to the difference in crop type, the use of fertilizer and tillage. In Wachiye et al., (2020), cropland was planted with annual crops of maize and beans, which were harvested by June, and thus less uptake of N by plants occurred afterwards. In addition, beans intercropped with maize may have played a role in legume N fixation in the cropland. Furthermore, the occasional use of manure reported in the study to improve soil N may have further led to greater N_2O fluxes.

Conversely, the slightly higher N_2O fluxes from site S1 could be a result of using sisal waste (about 40 t ha^{-1}) as a fertilizer during planting in November 2018. According to Echessa (2019), sisal leaf waste contains about 1.7 g kg^{-1} of nitrogen. The use of fertilizers has been reported to increase N in the soil (Houghton et al., 2012), and this explains the significantly higher mean NO_3^--N concentration in S1, which was more than ten times that of the other sites (Table 3). Similarly, the soil NH_4^+-N concentration was also significantly higher in S1 than the other sites.

We observed negative N_2O fluxes mostly during the dry season, an indication of N_2O uptake by the soils. This has also been reported from studies on similar tropical savannah soils under similarly dry conditions (Castaldi et al., 2006; Livesley et al., 2011; Wachiye et al., 2020). A possible explanation would be that due to the low N content observed at all sites and the low soil moisture in the dry seasons, atmospheric N_2O to diffuses into the soil and thus soil denitrifiers may use the N_2O as an N substrate in the absence of NO_2^- and NO_3^- (Rosenkranz et al., 2006).

4.3. Soil CH4 fluxes

Soil CH_4 fluxes showed no difference among the sisal stands. Most CH_4 flux values were below the LOD at all the sites. Soil CH_4 also displayed no seasonal variation, with no noticeable response to the onset of the wet season or dry season. However, the mean flux rates are comparable to those reported in other savannah ecosystems in Africa (Castaldi et al., 2006; Wachiye et al., 2020) and Australia (Livesley et al., 2011). We observed low soil C at all the sites, which affects soil microbes and methane oxidizers (Serrano-silva et al., 2014), thus providing a possible explanation for the lack of variation in CH_4 fluxes between the sites. Additionally, it has been reported that for methanogenesis to take place, soil should be under anaerobic conditions for some time to permit the establishment of methanogenic archaea (Serrano-Silva et al., 2014). Several studies have observed a shift from CH_4 uptake to CH4 emissions. For example, Castaldi et al. (2004) observed a change from CH_4 uptake to emissions at a W_S of 30% when moving from the dry season to the wet season in a temperate savannah. Another study by Brümmer et al., (2009) observed a shift from CH_4 uptake to CH_4 emissions at a soil W_S of 60–70% in Ghanaian savannah. However, in this study, W_S was always below 30%, even during the wet season with heavy rainfall at all sites, making W_S a key factor in regulating microbial activity, including methanogenic activity (Serrano-Silva et al., 2014). In spite of this, in the wet season, and especially in the short wet season, we occasionally observed short-lived CH_4 emissions in S8, S13 and S14, and it is possible that soil methanogenesis after the large rainfall events contributed. Nonetheless, for the other sites, the soil CH_4 flux in the wet season was similar to that in the dry season and no correlation was observed between CH_4 fluxes and either W_S or T_S.

4.4. Effects of stand properties on soil GHG fluxes

Soil F_S are controlled by a complex interaction of chemical, physical and biological factors in the soil including soil organic matter, soil texture, soil bulk density and soil pH (Smith et al. 2003). In the present study, the differences in soil texture (sand, silt and clay), SOC, BD, pH, NH_4-N and NO_3-N were of minor importance in explaining both cumulative soil CO_2 and N_2O fluxes (Table 3). Stepwise multiple regression yielded only one significant driving factor ($p < 0.01$), where cumulative N_2O fluxes were positively correlated with TN ($R = 0.71$; $p = 0.01$). This likely indicates that N availability for microorganisms plays a key role in determining soil N_2O fluxes at our site, since soil N_2O formation through nitrification and denitrification depends on N availability in the soil (Akiyama et al., 2000).

5. Conclusion

In this study, for the first time, we successfully measured soil GHG fluxes from a sisal chronosequence including young (1–3 years), mature (7–8 years) and old (13–14 years) stands in the Teita Sisal Estate, Kenya, in one of the largest sisal plantations in the world. Our results demonstrated low levels of soil N_2O and CH_4 with no or slight variation across sites and seasons, thus making their contribution to GHG emissions at the site scale negligible. Soil CO_2 fluxes, on the other hand, varied with stand age and water availability, i.e. season, indicating that soil moisture and vegetation are significant drivers of CO_2 fluxes. Compared to the control site, semi-natural bushland nearby grazed and browsed by animals, sisal estate contributed much higher CO_2 fluxes. Though we did not assess root biomass in this study, it is clear that a better understanding of the interactions between stand age and water availability will greatly advance the fundamental knowledge of the terrestrial C cycle in the tropics. In as much as, soil GHG fluxes from sisal plantations are only a minor contributor to agricultural GHG emissions in Kenya, these results are useful for policy making in development targeting climate-smart agricultural activities in the region. Nevertheless, the overall effects and contributions of agro-ecosystems to the overall carbon budget can only be established by further studies that observe both soil CO_2 emissions and soil CO_2 uptake.

Table 3
Soil characteristics at each study site (at a depth of 0–20 cm) in the Teita Sisal Estate and the surrounding bushland. The values in the table are means ± SE.

Site	pH	Bulk Density (g cm^{-3})	% N	% C	Clay (%)	Sand (%)	Silt (%)	μg NH_4^+-N g^{-1} DW	μg NO_3^--N g^{-1} DW
S1	6.5 ± 0.3	0.93 ± 0.03	0.09 ± 0.01	0.9 ± 0.2	29 ± 2	65.1 ± 1.0	5.9 ± 1.1	3.6 ± 1	24 ± 9
S2	7.9 ± 0.1	0.95 ± 0.04	0.09 ± 0.01	1.1 ± 0.3	26.9 ± 1.1	68.5 ± 1.5	4.6 ± 1.4	1.5 ± 0.4	4 ± 3
S3	5.5 ± 0.1	0.95 ± 0.09	0.08 ± 0.01	0.8 ± 0.1	26.3 ± 0.5	68.5 ± 0.5	5.3 ± 0.0	2.7 ± 1.2	1.7 ± 0.5
S7	7.2 ± 0.2	0.95 ± 0.02	0.07 ± 0.02	0.8 ± 0.2	26 ± 3	73 ± 2	1.9 ± 0.5	2.6 ± 0.8	1.2 ± 0.8
S8	6.2 ± 0.1	0.92 ± 0.08	0.10 ± 0.03	1.1 ± 0.3	35.6 ± 0.9	52.5 ± 0.6	11.9 ± 0.5	2.2 ± 0.9	0.6 ± 0.6
S13	7.7 ± 0.2	0.96 ± 0.09	0.10 ± 0.04	1.4 ± 0.9	26.3 ± 0.6	67.1 ± 0.1	6.6 ± 0.6	1.4 ± 0.3	1.2 ± 0.8
S14	7.2 ± 0.1	0.97 ± 0.06	0.08 ± 0.02	0.9 ± 0.2	20.9 ± 0.5	75.8 ± 0.5	3.3 ± 0.0	1.9 ± 0.3	4 ± 2
BL	6.7 ± 0.0	0.95 ± 0.06	0.09 ± 0.02	1.0 ± 0.1	31.6 ± 0.9	60.5 ± 1.4	7.9 ± 0.5	1.6 ± 0.8	4 ± 2

Data availability

The data associated with the manuscript can be obtained from https://figshare.com/articles/dataset/Soil_greenhouse_gas_emissions_from_a_sisal_chronosequence_in_Kenya/13213691

CRediT authorship contribution statement

Sheila Wachiye: Conceptualization, Data curation, Methodology, Formal analysis, Funding acquisition, Writing - original draft, Writing - review & editing. **Lutz Merbold:** Conceptualization, Formal analysis, Writing - review & editing. **Timo Vesala:** Writing - review & editing. **Janne Rinne:** Writing - review & editing. **Sonja Leitner:** Formal analysis, Writing - review & editing. **Matti Räsänen:** Writing - review & editing. **Ilja Vuorinne:** Formal analysis, Writing - review & editing. **Janne Heiskanen:** Formal analysis, Writing - review & editing. **Petri Pellikka:** Conceptualization, Writing - review & editing.

Declaration of Competing Interest

The authors declare that they have no conflicts of interest.

Acknowledgments

We acknowledge the management of Teita Sisal Estate for allowing us to conduct this research on the estate. Specifically, we would like to thank Mr Anthony Nielsen, Mr Jason Collette and Mr Emmanuel Mrombo for providing us with the necessary data and information relevant to this study. We thank the Taita Research Station of the University of Helsinki for technical and fieldwork support and the Mazingira Centre of the International Livestock Research Institute for technical support in the laboratory work. Specifically, we would like to thank Peter Mwasi, Darius Mwambala Kimuzi and Mwadime Mjomba for helping in data collection, as well as Paul Mutuo, Sheila Okoma, Margaret Muthoni and Collins Ouma for assistance with the laboratory work.

Financial support

The Schlumberger Foundation under the Faculty for the Future programme funded this study (4720995) for SW and PP. The work was conducted under the project “Environmental sensing of ecosystem services for developing a climate-smart landscape framework to improve food security in East Africa”, funded by the Academy of Finland (318645) for PP and TV. A research permit from NACOSTI (P/18/97336/26355) is acknowledged. LM and SL acknowledge the CGIAR Fund Council, Australia (ACIAR), Irish Aid, the European Union, IFAD, the Netherlands, New Zealand, the UK, USAID and Thailand for funding the CGIAR Research Program on Livestock. The research was carried out within the grant of the Tyumen region Government in accordance with the Program of the World-Class West Siberian Interregional Scientific and Educational Center (National Project "Nauka").

Supplementary materials

Supplementary material associated with this article can be found, in the online version, at doi:10.1016/j.agrformet.2021.108465.

References

Akiyama, H., Haruo, T., Takeshi, W., 2000. N_2O and NO emissions from soils after the application of different chemical fertilizers. Chemosphere 2 (3), 313–320. https://doi.org/10.1016/S1465-9972(00)00010-6 https://doi.org/.

Ardö, J., Meelis, M., Bashir, A.E., Elkhidir, H.A.M., 2008. Seasonal variation of carbon fluxes in a sparse savanna in Semi-Arid Sudan. Carbon Bal. Manag. 3 (December), 7. https://doi.org/10.1186/1750-0680-3-7 https://doi.org/.

Arias-Navarro, C., Díaz-Pinés, E., Kiese, R., Rosenstock, T.S., Rufino, M.C., Stern, D., Neufeldt, H., Verchot, L.V., Butterbach-Bahl, K., 2013. Gas pooling: a sampling technique to overcome spatial heterogeneity of soil carbon dioxide and nitrous oxide fluxes. Soil Biol. Biochem. 67 (December), 20–23. https://doi.org/10.1016/j.soilbio.2013.08.011 https://doi.org/.

Bahn, M., Schmitt, M., Siegwolf, R., Richter, A., Brüggemann, N., 2009. Does photosynthesis affect grassland soil-respired CO_2 and its carbon isotope composition on a diurnal timescale? New Phytol. 182 (2), 451–460. https://doi.org/10.1111/j.1469-8137.2008.02755.x https://doi.org/.

Bate, G.C., 1981. Nitrogen cycling in savanna ecosystems. Ecol. Bull. (33), 463–475.

Bingham, I.J., Stevenson, E.A., 1993. Control of root growth: effects of carbohydrates on the extension, branching and rate of respiration of different fractions of wheat roots. Physiol. Plant. 88 (1), 149–158. https://doi.org/10.1111/j.1399-3054.1993.tb01772.x https://doi.org/.

Boeckx, P., Van Nieuland, K., Van Cleemput, O., 2011. Short-term effect of tillage intensity on N_2O and CO_2 emissions. Agron. Sustainable Dev. 31 (3), 453–461. https://doi.org/10.1007/s13593-011-0001-9 https://doi.org/.

Bremer, D.J., Ham, M.J., Owensby, E.C., Knapp, A.K., 1998. Responses of soil respiration to clipping and grazing in a Tallgrass Prairie. J. Environ. Qual. 27 (6), 1539–1548. https://doi.org/10.2134/jeq1998.00472425002700060034x https://doi.org/.

Broeren, M.L., Dellaert, S.N.C., Cok, B., Patel, M.K., Worrell, E, Shen, L., 2017. Life cycle assessment of sisal fibre – exploring how local practices can influence environmental performance. J. Clean. Prod. 149 (April), 818–827. https://doi.org/10.1016/j.jclepro.2017.02.073 https://doi.org/.

Brümmer, C., Brüggemann, N., Butterbach-Bahl, K., Falk, U., Szarzynski, J., Vielhauer, K., Wassmann, R., Papen, H., 2008. Soil-atmosphere exchange of N_2O and NO in near-natural savanna and agricultural land in Burkina Faso (W. Africa). Ecosystems 11 (4), 582–600. https://doi.org/10.1007/s10021-008-9144-1 https://doi.org/.

Carbone, M.S., Still, C.J., Ambrose, R.A., Dawson, E.T., Williams, P.A., Boot, M.C., Schaeffer, M.S., Schimel, P.J., 2011. Seasonal and episodic moisture controls on plant and microbial contributions to soil respiration. Oecologia 167 (1), 265–278. https://doi.org/10.1007/s00442-011-1975-3 https://doi.org/.

Castaldi, Simona, Ermice, Antonella, Strumia, Sandro, 2006. Fluxes of N_2O and CH_4 from soils of savannas and seasonally-dry ecosystems. J. Biogeogr. 33 (3), 401–415. https://doi.org/10.1111/j.1365-2699.2005.01447.x https://doi.org/.

Castaldi, S., Ariangelo, R.D., John, G., Nina, N., Ruben, M., José, S., 2004. Nitrous Oxide and methane fluxes from soils of the orinoco savanna under different land uses. Glob. Change Biol. 10 (11), 1947–1960. https://doi.org/10.1111/j.1365-2486.2004.00871.x https://doi.org/.

Christiansen, J.R., Korhonen, F.J., Juszczak, R., Giebels, M., Pihlatie, M., 2011. Assessing the effects of chamber placement, manual sampling and headspace mixing on CH_4 fluxes in a laboratory experiment. Plant Soil 343 (1), 171–185. https://doi.org/10.1007/s11104-010-0701-y https://doi.org/.

Cruz, M.V., Dierig, D.A., 2015. Industrial Crops: Breeding for Bioenergy and Bioproducts. Industrial Crops. Breeding for Bioenergy and Bioproducts. https://doi.org/10.1007/978-1-4939-1447-0 https://doi.org/.

DAFF, 2015. Department of Agriculture, Forestry and Fisheries, Republic of South Africa. Sisal, Production Guideline. http://www.daff.gov.za/Daffweb3/Portals/0/Brochures%20and%20Production%20guidelines/Sisal%20Production%20Guideline.pdf.

Davidson, E.A., Belk, E., Boone, D.R., 1998. Soil water content and temperature as independent or confounded factors controlling soil respiration in a temperate mixed hardwood forest. Global Change Biol. 4 (2), 217–227. https://doi.org/10.1046/j.1365-2486.1998.00128.x https://doi.org/.

Davidson, E.A., Keller, M., Erickson, E.H., Verchot, V.L., Veldkamp, E., 2000. Testing a conceptual model of soil emissions of nitrous and nitric oxides using two functions based on soil nitrogen availability and soil water content, the hole-in-the-pipe model characterizes a large fraction of the observed variation of nitric oxide and nitrous oxide emissions from soils. Bioscience 50 (8), 667–680. https://doi.org/10.1641/0006-3568(2000)050[0667:TACMOS]2.0.CO;2 https://doi.org/.

Didan, K., Munoz, A. B., Solano, R., Huete, A., 2015. MODIS vegetation index user’s guide (MOD13 series) version 3.00, June 2015 (Collection 6). https://vip.arizona.edu/documents/MODIS/MODIS_VI_UsersGuide_June_2015_C6.pdf.

Echessa, A.C., 2019. Variation of plant macronutrients in sisal (Agavesisalana) leaves biomass, 5.

Ewel, K.C., Cropper Jr, W.P., Gholz, L.H., 1987. Soil CO_2 evolution in Florida slash pine plantations. I. Changes through time. Can. J. For. Res. 17 (4), 325–329. https://doi.org/10.1139/x87-054 https://doi.org/.

FAO, 2012. Future fibres. Sisal. http://www.fao.org/economic/futurefibres/fibres/sisal/en/ (accessed March, 2019).

Fang, C., Moncrieff, J., Gholz, H., Clark, K., 1998. Soil CO_2 efflux and its spatial variation in a florida slash pine plantation. Plant Soil 205 (2), 135–146. http://www.paper.edu.cn/scholar/showpdf/MUj2QN5IOTD0gxeQh.

Gao, J., Zhang, Y., Song, Q., Lin, Y., Zhou, R., Dong, Y., Zhou, L., 2019. Stand age-related effects on soil respiration in rubber plantations (Hevea Brasiliensis) in Southwest China. Eur. J. Soil Sci. 70 (6), 1221–1233. https://doi.org/10.1111/ejss.12854 https://doi.org/.

Githire, R.W., 1987. An economic analysis of the Kenyan sisal industry, 142. http://erepository.uonbi.ac.ke/bitstream/handle/11295/23831/Githire%20Ruth%20K_An%20Economic%20Analysis%20Of%20The%20Kenyan%20Sisal%20Industry(2).pdf?sequence=3.

Grace, J., José., José San, Meir, P., Miranda, H.S., Montes, R.A., 2006. Productivity and carbon fluxes of tropical savannas. J. Biogeogr. https://doi.org/10.1111/j.1365-2699.2005.01448.x. March 1, 2006https://doi.org/.

Grover, S.P.P., Livesley, S.J., Hutley, L.B., Jamali, H., Fest, B., Beringer, J., Butterbach-Bahl, K., Arndt, S.K., 2012. Land use change and the impact on greenhouse gas

exchange in North Australian savanna soils. Biogeosciences 9 (January), 423–437. https://doi.org/10.5194/bg-9-423-2012 https://doi.org/.

Hickman, J.E., Palm, A.C., Mutuo, K.P., Melillo, J.M., Tang, J., 2014. Nitrous oxide (N_2O) emissions in response to increasing fertilizer addition in Maize (Zea Mays L.) agriculture in Western Kenya. Nutr. Cycling Agroecosyst. 100, 177–187. https://doi.org/10.1007/s10705-014-9636-7 https://doi.org/.

Högberg, P., Nordgren, A., Buchmann, N., Taylor, A.F., Ekblad, A., Högberg, M.N., Nyberg, G., Ottosson-Löfvenius, M., Read, D.J., 2001. Large-scale forest girdling shows that current photosynthesis drives soil respiration. Nature 411 (6839), 789–792. https://doi.org/10.1038/35081058 https://doi.org/.

Hood-Nowotny, R., Umana, H.N., Inselbacher, E., Oswald- Lachouani, P., Wanek, W., 2010. Alternative methods for measuring inorganic, organic, and total dissolved nitrogen in soil. Soil Sci. Soc. Am. J. 74 (3), 1018–1027. https://doi.org/10.2136/sssaj2009.0389 https://doi.org/.

Houghton, R.A., House, J.I., Pongratz, J., Van der Werf, G.R., DeFries, D.S., Hansen, M. C., Le Quéré, C., Ramankutty, N., 2012. Carbon emissions from land use and land-cover change. Biogeosciences 9 (12), 5125–5142. https://doi.org/10.5194/bg-9-5125-2012 https://doi.org/.

Huete, A.R., Liu, H.Q., Batchily, K., van Leeuwen, W., 1997. A comparison of vegetation indices over a global set of TM images for EOS-MODIS. Remote Sens. Environ. 59 (3), 440–451. https://doi.org/10.1016/S0034-4257(96)00112-5 https://doi.org/.

Hutchinson, G.L., Mosier, A.R., 1981. Improved soil cover method for field measurement of nitrous oxide fluxes 1. Soil Sci. Soc. Am. J. 45 (2), 311–316. https://doi.org/10.2136/sssaj1981.03615995004500020017x https://doi.org/.

Huxman, T.E., Snyder, K.A, Tissue, D.A., Leffler, J., Ogle, K., Pockman, W.T, Sandquist, D.R., Potts, D.L., Schwinning, S., 2004. Precipitation pulses and carbon fluxes in semiarid and arid ecosystems. Oecologia 141 (2), 254–268. https://doi.org/10.1007/s00442-004-1682-4 https://doi.org/.

IPCC, 2013: Climate change: the physical science basis. 2013. Rationale reference. European Environment Agency. Accessed November 29, 2018. https://www.eea.europa.eu/data-and-maps/indicators/glaciers-2/ipcc-2013-climate-change-2013.

Kimaro, D.N., Msanya, M.B., Takamura, Y.T., 1994. Review of Sisal Production and Research in Tanzania. https://doi.org/10.14989/68124 https://doi.org/.

Klopatek, J.M., 2002. Belowground carbon pools and processes in different age stands of douglas-fir. Tree Physiol. 22 (2–3), 197–204. https://doi.org/10.1093/treephys/22.2-3.197 https://doi.org/.

Law, B.E., Sun, O.J., Campbell, J., Van Tuyl, S., Thornton, P.E., 2003. Changes in carbon storage and fluxes in a chronosequence of ponderosa pine. Global Change Biol. 9 (4), 510–524. https://doi.org/10.1046/j.1365-2486.2003.00624.x https://doi.org/.

Li, X., Guo, D., Zhang, C., Niu, D., Fu, H., Wan, C., 2018. Contribution of root respiration to total soil respiration in a semi-arid grassland on the Loess Plateau, China. Sci. Total Environ. 627 (June), 1209–1217. https://doi.org/10.1016/j.scitotenv.2018.01.313 https://doi.org/.

Li, Y., Mai, Y., Ye, L., 2000. Sisal fibre and its composites: a review of recent developments. Compos. Sci. Technol. 60 (11), 2037–2055. https://doi.org/10.1016/S0266-3538(00)00101-9 https://doi.org/.

Livesley, S.J., Grover, S., Hutley, L.B., Jamali, H., Butterbach-Bahl, K., Fest, B., Beringer, J., Arndt, S.K., 2011. Seasonal variation and fire effects on CH_4, N_2O and CO_2 exchange in savanna soils of Northern Australia. Agric. For. Meteorol. 151 (11), 1440–1452. https://doi.org/10.1016/j.agrformet.2011.02.001 https://doi.org/.

Ludwig, J., Meixner, F.X., Vogel, B., Förstner, J., 2001. Soil-air exchange of nitric oxide: an overview of processes, environmental factors, and modeling studies. Biogeochemistry 52 (3), 225–257.

Lüttge, Ulrich, 2004. Ecophysiology of crassulacean acid metabolism (CAM). Ann. Bot. (Lond.) 93 (6), 629–652. https://doi.org/10.1093/aob/mch087 https://doi.org/.

Manzoni, S., Katul, G., 2014. Invariant soil water potential at zero microbial respiration explained by hydrological discontinuity in dry soils. Geophys. Res. Lett. 41 (20), 7151–7158. https://doi.org/10.1002/2014GL061467 https://doi.org/.

Marteau, R., Sultan, B., Moron, V., Alhassane, A., Baron, C., Traoré, B.S., 2011. The onset of the rainy season and farmers' sowing strategy for pearl millet cultivation in Southwest Niger. Agric. For. Meteorol. 151 (10), 1356–1369. https://doi.org/10.1016/j.agrformet.2011.05.018 https://doi.org/.

Merbold, L., Ardo, J., Arneth, A., Scholes, R.J., Nouvellon, Y., de Grandcourt, A., Archibald, S., 2009. Precipitation as driver of carbon fluxes in 11 African ecosystems, 15. https://bg.copernicus.org/articles/6/1027/2009/bg-6-1027-2009.pdf.

Muñoz, C., Paulino, L., Monreal, C., Zagal, E., 2010. Greenhouse gas (CO_2 and N_2O) emissions from soils: a review. Chil. J. Agric. Res. 70 (3) https://doi.org/10.4067/S0718-58392010000300016 https://doi.org/.

Njagi, K., 2018. FEATURE-plastic ban raises hopes for Kenya's sisal farmers. Reuters. June 22, 2018. https://www.reuters.com/article/kenya-farming-pollution-idINL8N1TM2I1.

Nobel, P.S., Sanderson, J., 1984. Rectifier-like activities of roots of two desert succulents. In . https://doi.org/ 10.1093/jxb/35.5.727.

Nobel, P.S., Quero, E., 1986. Environmental productivity indices for a chihuahuan desert cam plant, Agave Lechuguilla. Ecology 67 (1), 1–11. https://doi.org/10.2307/1938497 https://doi.org/.

Oertel, C., Matschullat, J., Zurba, K., Zimmermann, F., Erasmi, S., 2016. Greenhouse gas emissions from soils—a review. Chem. Erde 76 (3), 327–352. https://doi.org/10.1016/j.chemer.2016.04.002 https://doi.org/.

Palta, J.A., Nobel, P.S., 1989. Root respiration for agave deserti: influence of temperature, water status and root age on daily patterns. J. Exp. Bot. 40 (211), 181–186.

Parkin, T.B., Venterea, R.T., Hargreaves, S.K., 2012. Calculating the detection limits of chamber-based soil greenhouse gas flux measurements. J. Environ. Qual. 41 (3), 705. https://doi.org/10.2134/jeq2011.0394 https://doi.org/.

Pellikka, P.K.E., Heikinheimo, V., Hietanen, J., Schäfer, E., Siljander, M., Heiskanen, J., 2018. Impact of land cover change on aboveground carbon stocks in Afromontane landscape in Kenya. Appl. Geogr. 94, 178–189. https://www.sciencedirect.com/science/article/pii/S0143622817309979.

Pelster, D., Rufino, M., Rosenstock, T., Mango, J., Saiz, G., Diaz-Pines, E., Baldi, G., Butterbach-Bahl, K., 2017. Smallholder farms in Eastern African Tropical highlands have low soil greenhouse gas fluxes. Biogeosciences 14 (1), 187–202. https://doi.org/10.5194/bg-14-187-2017 https://doi.org/.

Pinto, A.S., Bustamante, M.M.C., Kisselle, K., Burke, R., Zepp, R., Viana, L.T., Varella, R. F., Molina, M., 2002. Soil emissions of N_2O, NO, and CO_2 in Brazilian Savannas: effects of vegetation type, seasonality, and prescribed fires. J. Geophys. Res. 107 (D20) https://doi.org/10.1029/2001JD000342. LBA 57-1-LBA 57-9https://doi.org/.

Raich, J.W., Tufekcioglu, A., 2000. Vegetation and soil respiration: correlations and controls. Biogeochemistry 48 (1), 71–90. https://link.springer.com/article/10.1023/A:1006112000616.

Roby, M.C., Scott, R.L., Barron-Gafford, G.A., Hamerlynck, E.P., Moore, D.J.P., 2019. Environmental and vegetative controls on soil CO_2 Efflux in three semiarid ecosystems. Soil Syst. 3 (1), 6. https://doi.org/10.3390/soilsystems3010006 https://doi.org/.

Rochette, P., 2011. Towards a standard non-steady-state chamber methodology for measuring soil N_2O emissions. Anim. Feed Sci. Technol. 166–167 (June), 141–146. https://doi.org/10.1016/j.anifeedsci.2011.04.063. Special Issue: Greenhouse Gases in Animal Agriculture - Finding a Balance between Food and Emissionshttps://doi.org/.

Rochette, P., Bertrand, N., 2003. Soil air sample storage and handling using polypropylene syringes and glass vials. Can. J. Soil Sci. 83 (5), 631–637. https://doi.org/10.4141/S03-015 https://doi.org/.

Rosenstock, T.S., Mpanda, M., Pelster, D.E., Butterbach-Bahl, K., Rufino, M.C., Thiong'o, M., Mutuo, P., 2016. Greenhouse gas fluxes from agricultural soils of Kenya and Tanzania: GHG fluxes from agricultural soils of East Africa. J. Geophys. Res. 121 (6), 1568–1580. https://doi.org/10.1002/2016JG003341 https://doi.org/.

Saiz, G., Byrne, K., Butterbach-Bahl, K., Kiese, R., Blujdea, V., Edward, P.F., 2006. Stand age-related effects on soil respiration in a first rotation sitka spruce chronosequence in Central Ireland. Global Change Biol. 12 (6), 1007–1020. https://doi.org/10.1111/j.1365-2486.2006.01145.x https://doi.org/.

Scholes, R.J., Ward, D.E., Justice, C.O., 1996. Emissions of trace gases and aerosol particles due to vegetation burning in southern hemisphere Africa. J. Geophys. Res. 101 (D19), 23677–23682. https://doi.org/10.1029/95JD02049 https://doi.org/.

Serrano-silva, N., Sarria-guzmán, Y., Dendooven, Y., Luna-guido, M., 2014. Methanogenesis and methanotrophy in soil: a review. Pedosphere 24 (3), 291–307. https://doi.org/10.1016/S1002-0160(14)60016-3 https://doi.org/.

Sigau, C.U., Hamid, A.H., 2018. Soil CO2 efflux of oil palm and rubber plantation in 6-year- old and 22-year-old chronosequence,16. http://www.myjurnal.my/filebank/published_article/76409/22.pdf.

Smith, D.R., Townsend, T.J., Choy, A.W.K., Hardy, I.C.W., Sjögersten, S., 2012. Short-term soil carbon sink potential of oil palm plantations. GCB Bioenergy 4 (5), 588–596. https://doi.org/10.1111/j.1757-1707.2012.01168.x https://doi.org/.

Smith, K.A., Ball, T., Conen, F., Dobbie, K.E., Massheder, J., Rey, A., 2003. Exchange of greenhouse gases between soil and atmosphere: interactions of soil physical factors and biological processes. Eur. J. Soil Sci. 54 (4), 779–791. https://doi.org/10.1046/j.1351-0754.2003.0567.x https://doi.org/.

Søe, A.R.B., Giesemann, A., Anderson, T., Weigel, H., Buchmann, N., 2004. Soil respiration under elevated CO_2 and its partitioning into recently assimilated and older carbon sources. Plant Soil 262 (1), 85–94. https://doi.org/10.1023/B:PLSO.0000037025.78016.9b https://doi.org/.

Tang, X., Liu, S., Zhou, G., Zhang, D., Zhou, C., 2006. Soil-atmospheric exchange of CO_2, CH_4, and N_2O in three subtropical forest ecosystems in Southern China. Global Change Biol. 12 (3), 546–560. https://doi.org/10.1111/j.1365-2486.2006.01109.x https://doi.org/.

Toland, D.E., Zak, D.R., 1994. Seasonal patterns of soil respiration in intact and clear-cut northern hardwood forests. Can. J. Forest Res. (Canada). https://agris.fao.org/agris-search/search.do?recordID=CA9502712.

Topp, E., Pattey, E., 1997. Soils as sources and sinks for atmospheric methane. Can. J. Soil Sci. 77 (2), 167–177. https://doi.org/10.4141/S96-107 https://doi.org/.

Tsuda, S., 2019. Taita Basket branding project in Kenya, 18. https://www.wipo.int/edocs/mdocs/africa/en/wipo_ip_bbk_19/wipo_ip_bbk_19_t_3.pdf.

Valentini, R., Arneth, A., Bombelli, A., Castaldi, S., Cazzolla Gatti, R., Chevallier, F., Ciais, P., et al., 2014. A full greenhouse gases budget of Africa: synthesis, uncertainties, and vulnerabilities. Biogeosciences 11 (2), 381–407. https://doi.org/10.5194/bg-11-381-2014 https://doi.org/.

Vuorinne, I., Heiskanen, J., Mwangala, L., Maghenda, M., Pellikka, P.K.E., 2021a. Allometry, biomass and productivity of *Agave sisalana* leaves. Submitted. https://helda.helsinki.fi/bitstream/handle/10138/316946/Vuorinne_Ilja_Pro_Gradu_2020.pdf.

Vuorinne, I., Heiskanen, J., Pellikka, P., 2021b. Assessing leaf biomass of Agave sisalana using Sentinel-2 vegetation indices. Remote Sens. In print.

Wachiye, S., Merbold, L., Vesala, T., Rinne, J., Räsänen, M., Leitner, S., Pellikka, P., 2020. Soil greenhouse gas emissions under different land-use types in savanna ecosystems of Kenya. Biogeosciences 17 (8), 2149–2167. https://doi.org/10.5194/bg-17-2149-2020 https://doi.org/.

Wang, C., Bond-Lamberty, B., Gower, S.T., 2002. Soil surface CO_2 flux in a boreal black spruce fire chronosequence. J. Geophys. Res. 107 (D3) https://doi.org/10.1029/2001JD000861. WFX 5-1-WFX 5-8https://doi.org/.

Wang, W., Zeng, W., Chen, W., Yang, Y., Zeng, H., 2013. Effects of forest age on soil autotrophic and heterotrophic respiration differ between evergreen and deciduous

forests. PLoS One 8 (11), e80937. https://doi.org/10.1371/journal.pone.0080937 https://doi.org/.

Wanyama, I., Pelster, D.E., Butterbach-Bahl, K., Verchot, L.V., Martius, C., Rufino, M.C., 2019. Soil carbon dioxide and methane fluxes from forests and other land use types in an African tropical montane region. Biogeochemistry 143 (2), 171–190. https://doi.org/10.1007/s10533-019-00555-8 https://doi.org/.

Wiseman, P.E., Seiler, J.R., 2004. Soil CO_2 efflux across four age classes of plantation loblolly pine (Pinus Taeda L.) on the virginia piedmont. Forest Ecol. Manag. 192 (2), 297–311. https://doi.org/10.1016/j.foreco.2004.01.017 https://doi.org/.

Yan, M., Zhang, X., Zhou, G., Gong, J., You, X., 2011. Temporal and spatial variation in soil respiration of poplar plantations at different developmental stages in Xinjiang, China. J. Arid Environ. 75 (1), 51–57. https://doi.org/10.1016/j.jaridenv.2010.09.005 https://doi.org/.

Yang, X., Cushman, J.C., Borland, A.M., Edwards, E.J., Wullschleger, S.D., Tuskan, G.A., Owen, N.A., 2015. A roadmap for research on crassulacean acid metabolism (CAM) to enhance sustainable food and bioenergy production in a hotter, Drier World. New Phytol. 207 (3), 491–504. https://doi.org/10.1111/nph.13393 https://doi.org/.

Yin, S., Zhang, X., Pumpanen, J., Shen, G., Xiong, F., Liu, C., 2016. Seasonal variation in soil greenhouse gas emissions at three age-stages of dawn redwood (Metasequoia Glyptostroboides) stands in an Alluvial Island, Eastern China. Forests 7 (11), 256. https://doi.org/10.3390/f7110256 https://doi.org/.

Zhao, X., Li, F., Zhang, W., Ai, Z., Shen, H., Liu, X., Cao, J., Manevski, K., 2016. Soil respiration at different stand ages (5, 10, and 20/30 Years) in Coniferous (Pinus Tabulaeformis Carrière) and Deciduous (Populus Davidiana Dode) plantations in a Sandstorm Source Area. Forests 7 (8), 153. https://doi.org/10.3390/f7080153 https://doi.org/.

Zheng, Z., Yu, G., Fu, Y., Wang, Y., Sun, X., Wang, Y., 2009. Temperature sensitivity of soil respiration is affected by prevailing climatic conditions and soil organic carbon content: a trans-China based case study. Soil Biol. Biochem. 41 (7), 1531–1540. https://doi.org/10.1016/j.soilbio.2009.04.013 https://doi.org/.